Hindawi
Journal of Nanotechnology
Volume 2022, Article ID 2779237, 24 pages
https://doi.org/10.1155/2022/2779237

Review Article

Plant-Mediated Green Synthesis of Ag NPs and Their Possible Applications: A Critical Review

Darbin Kumar Poudel,[1,2] **Purushottam Niraula**,[2] **Himal Aryal**,[2] **Biplab Budhathoki**,[2] **Sitaram Phuyal**,[2] **Rishab Marahatha**,[2] **and Kiran Subedi**[3]

[1]*Analytica Research Center, Kritipur, Kathmandu, Nepal*
[2]*Central Department of Chemistry, Tribhuvan University, Kirtipur, Kathmandu, Nepal*
[3]*North Carolina Agricultural and Technical State University, Greensboro, USA*

Correspondence should be addressed to Darbin Kumar Poudel; darkwine51@gmail.com

Received 8 September 2021; Revised 30 January 2022; Accepted 17 February 2022; Published 16 March 2022

Academic Editor: Brajesh Kumar

The potential applications of Ag NPs are exciting and beneficial in a variety of fields; however, there is less awareness of the new risks posed by inappropriate disposal of Ag NPs. The Ag NPs have medicinal, plasmonic, and catalytic properties. The Ag NPs can be prepared via physical, chemical, or biological routes, and the selection of any specific route depends largely on the end-use. The downside of a physical and chemical approach is that it requires a wide space, high temperature, high temperature for a longer time to preserve the thermal stability of synthesized Ag NPs, and the use of toxic chemicals. Although these methods produce nanoparticles with high purity and well-defined morphology, it is critical to develop cost-effective, energy-efficient, and facile route, such as green synthesis; it suggests the desirable use of renewable resources by avoiding the use of additional solvents and toxic reagents in order to achieve the ultimate goal. However, each method has its pros and cons. The synthesized Ag NPs obtained using the green approach have larger biocompatibility and are less toxic towards the biotic systems. However, identifying the phytoconstituents that are responsible for nanoparticle synthesis is difficult and has been reported as a suitable candidate for biological application. The concentration of the effective bioreducing phytoconstituents plays a crucial role in deciding the morphology of the nanoparticle. Besides these reaction times, temperature, pH, and concentration of silver salt are some of the key factors that determine the morphology. Hence, careful optimization in the methodology is required as different morphologies have different properties and usage. It is due to which the development of methods to prepare nanoparticles effectively using various plant extracts is gaining rapid momentum in recent days. To make sense of what involves in the bioreduction of silver salt and to isolate the secondary metabolites from plants are yet challenging. This review focuses on the contribution of plant-mediated Ag NPs in different applications and their toxicity in the aquatic system.

1. Introduction

Nanomaterials are generally defined as structures that have at least one dimension below 100 nm. Recently, there has been an increased demand for nanomaterials because of their widespread application in multidisciplinary fields. The global market of nanoparticles is expected to reach USD 16.8 billion, and commercialized Ag NPs contribute to 17.86% by 2021 [1].

The green synthetic approach has been proposed as a cost-effective, energy-efficient, facile, and environmentally friendly method for the preparation of nanomaterials as the use of nontoxic bioreducing agents provides alternative solutions to various environmentally conscious products. Green synthesized nanoparticles have a high surface area to volume ratio, biocompatible surface properties, less toxicity, and chemical stability. Multifunctional applications such as antibacterial [2, 3], antiviral [4], antifungal [5], anti-inflammatory [6], antidiabetic [7], anticancer [8], metal sensing [9], catalysis [10], and dye degradation [11] are some of the reasons why Ag NPs are emerging as the most

fascinating and studied nanomaterials among other metallic nanoparticles.

Despite these applications, some of their hazardous effects, especially in the aquatic biotic system when inappropriately disposed, cannot be underestimated [12]. Tons of Ag NPs have been reported to be disposed into the aquatic environment annually [13]. The toxicity of Ag NPs depends on the physicochemical properties of nanoparticles as they differ from bulk material due to the higher surface area to volume ratio which enhances their reactivity [14].This increased reactivity also translates towards biological systems via the food chain, which raises concern regarding the Ag NPs toxicity that exhibits cytotoxic, genotoxic, and hepatotoxic properties in any tropical level due to generation of reactive oxygen species (ROS) [15] or dissolution induced release of silver ion [16]. The nanoparticles showed size- and dose-dependent cytotoxicity towards macrophages [17] and T cells [18]. Slightly lesser toxicity of Ag NPs in comparison to Ag+ ions was reported [19] in *Escherichia coli*. Ag NPs displayed cytotoxicity through apoptosis both in *in vitro* and *in vivo* in the human epithelial cells [20]. The toxicity of green synthesized Ag NPs has been observed to depend on capping agent and surface functionalization showing less toxicity, which increases their potential for various biomedical applications [21].

Several reviews have been published on the biogenesis/chemical/physical synthesis and characterization of Ag NPs. In this paper, we have attempted to provide comprehensive detail of plant-mediated Ag NPs applications and their toxicity in the aquatic system.

2. Properties of Ag NPs

Green synthesized Ag NPs display novel and size-related physicochemical properties. In addition to that they also exhibit optical properties such as loss of the optical frequency during the surface plasmon propagation, wide absorption of the visible and far infrared region of the light, and surface-enhanced Raman scattering (SERS). These particles also have high electrical and thermal conductivity, high reactivity, and excellent catalytic and biological activities. The biological activity of Ag NPs depends on various elements including surface chemistry, shape and size, size distribution, capping/stabilizing agents, and agglomeration to name a few [22]. Because of these properties, they can be utilized for a variety of applications.

3. Methods of Synthesis of Ag NPs

The synthetic procedure for Ag NPs can be broadly categorized as top-down and bottom-up strategies. In the top-down approach, bulk materials are disassembled to create the nanostructures needed, whereas in the bottom-up method, single atoms and molecules are integrated into larger nanostructures [23]. Moreover, the synthesis strategy can be categorized as physical, chemical, and biological approaches. Since this review is for biological methods, the other methods are only briefly discussed here.

3.1. Physical Methods. The physical process involves two methods: evaporation-condensation and laser ablation. Evaporation-condensation is an inert gas-phase route that uses a horizontal tube furnace at atmospheric pressure to create nanoparticles. Throughout the center of the tube, the furnace contains a boat with synthesizing metal source material that is vaporized into the carrier gas. This technique has been used to synthesize nanoparticles, such as Au [24] and PbS [25]. An inert gas condensation system was used to synthesize Ag NPs using liquid helium in the process chamber, and the particle size ranged from 9 to 32 nm [26]. Some disadvantages of this technique include the need for a large space, high temperature, and high temperature for a longer period of time in order to retain the thermal stability of produced Ag NPs.

In laser ablation, a portion of the firm target material in solution is irradiated by using a laser of suitable wavelength, resulting in the formation of nanoparticles. Ag NPs have been prepared by irradiating a target silver in pure water with a 532 nm laser beam [27]. Following laser irradiation, the liquid can only comprise the intended solid nanoparticles and no other ions, compounds, reducing agents, etc. [28]. Laser ablation synthesis of nanoparticles is clean and uncontaminated, as this process uses mild surfactants in the solvent without any other toxic or hazardous chemical reagents. Spherical, uniformly dispersed, and homogeneous sized Ag NPs are prepared by spark ablation processes [29]. Physical approaches, which are capable of producing nanoparticles with higher purity and well-defined morphologies, are costly.

3.2. Chemical Methods. Chemical reduction is one of the most widely employed techniques for the synthesis of Ag NPs that uses both inorganic and organic reducing agents. Silver nitrate is used as a precursor, and various reducing agents such as sodium citrate, ascorbate, sodium borohydride, elemental hydrogen, polyol cycle, Tollens' reagent, N,N-dimethylformamide, poly(ethylene glycol)-block copolymers, hydrazine, and ammonium formate are used to reduce Ag^+ ion [30]. Spherical Ag NPs are obtained by the use of reducing agents (trisodium citrate and sodium borohydride), and polyvinyl pyrrolidone act as a stabilizing agent [31]. The morphology of the product nanoparticles highly depends on the kind of reducing agent/stabilizing agents used and reaction conditions [32]. The disadvantage of chemical method is that toxic chemicals may be harmful to biotic components.

3.3. Biological Methods. Advancing biological synthesis over chemical and physical processes is environmentally sustainable, cost-effective, and quickly scaled up for the production of nanoparticles on a wide scale; however, each method has its pros and cons. The biological approach is a less expensive, biocompatible, cleaner, nontoxic, and often single-step process that uses secondary metabolites (phenolics, flavonoids, terpenes, carbohydrates, etc.) as well as biomolecules such as DNA, protein, and enzymes spread in fungi, microbes, algae, and plants as reducing,

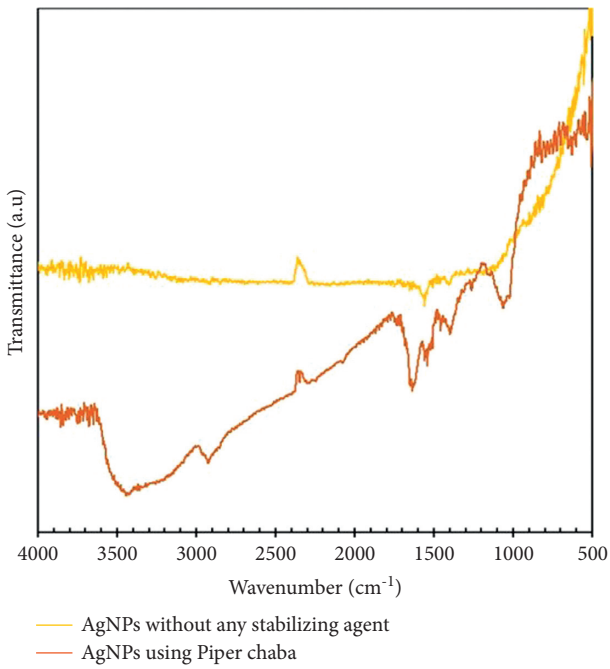

FIGURE 1: Fourier transform infrared (FTIR) spectra of Ag NPs synthesized using $AgNO_3$ (1 mM, 40 mL) and *Piper chaba* extract (100 g/L, 2 mL) after the reaction for 1 h at 60°C and pH = 7, and Ag NPs synthesized without capping agent reduced by $NaBH_4$ [59] (open access and reprinted under CC BY 4.0).

capping, and stabilizing agents. Biomolecule-mediated synthesis (DNA, protein, and enzymes) provides specific nucleation site during nanoparticle synthesis, resulting in uniform sized nanoparticles that are selective and sensitive to biomolecular targets and have a wide range of biomedical applications. These techniques, however, are extremely susceptible to environmental conditions such as temperature and pH [33–36]. The size of synthesized nanoparticles is also affected by the molar ratio of silver salt and biomolecules. DNA-mediated nanoparticles showed good antibacterial activity [37–39], and protein-mediated nanoparticles showed sensing application on spike proteins [40].

Bacterial species are sources of bioreducing secondary metabolites for silver salts, and *Bacillus amyloliquefaciens* and *Bacillus subtilis* [41], *Pseudomonas aeruginosa* [42], *Escherichia coli* [43], and *Acinetobacter calcoaceticus* [44] have also been used in the synthesis of Ag NPs. However, microbe-controlled synthesis is not industrially feasible because of the high aseptic criteria and their management. Therefore, the usage of plant extracts for this purpose has proven as a facile route over microorganisms owing to the simplicity, least biohazardous, and the nonrequirement of cell culture maintenance. Plants are readily accessible and have a broad variety of active functional groups and contain varieties of secondary metabolites such as polysaccharides, tannins, saponins, phenolics, terpenoids, flavonoids, alkaloids, sugars, enzymes, carbohydrates, and amino acids that can be useful in reducing, capping, and stabilizing Ag NPs observed in FTIR analysis [30]. Plants such as *Lippia citriodora* [45], *Terminalia arjuna* [11], *Cannabis sativa* [46], *Salvia officinalis* [47], *Jatropha curcas* seed [48], *Caesalpinia coriaria* [49], *Artemisia nilagirica* [50], *Parkia speciosa* [51], *Cinnamon zeylanicum* [52], *Lysiloma acapulcensis* [53], *Euphorbia prostrata* [54], *Cocos nucifera* coir [55], *Camellia sinensis* [56], *Sideritis argyrea* [57], and *Ipomoea staphylina* [58] have been used for the synthesis of Ag NPs Figure 1.

4. Plant-Mediated Ag NPs and Factors Affecting the Formation of Ag NPs

Biocompatible and nontoxic synthesis of functional nanoparticles assumes a vital job in the field of nanotechnology. It has been portrayed as a facile synthetic method as it is environmentally friendly, safe, and of solvent-free nature and avoids toxins. Different secondary metabolites from plants serve as reducing, stabilizing, and capping agents. Different plants produce a different class of secondary metabolites from having a certain degree of bioreduction potential capability of donating electrons for the reduction of Ag^+ ions to Ag^0 that decides the morphology, size, and yield of Ag NPs [60]. For nanotransformation of silver salt, electrons are supposed to be derived from dehydrogenation of acids and alcohols/phenols in hydrophytes, keto to enol conversions in mesophytes, or both mechanisms in xerophyte plants. Upon the release of two electrons from bioreducing secondary metabolites, it leads to the reduction of two silver ions which cluster together resulting the formation of Ag NPs [61–63]. The size of the nanoparticle plays a crucial role in determining its properties. Almost all plant-mediated Ag NPs have a spherical shape [64, 65]. Along with the nature and concentration of the secondary metabolites, distinctive factors such as pH, temperature, reduction time, the ratio of the concentration of silver salts, and plant extract also influence the formation of nanoparticles [66, 67].

pH is a major parameter that determines the uniformity and size of Ag NPs. The change in the pH of the reaction mixture and the plant extract can alter the shape and size of the nanoparticles. There is an inverse correlation between the size of nanoparticles formed and the pH of the reaction mixture [68]. However, at acidic conditions, almost no Ag NPs were produced as confirmed by the absence of a strong surface plasmon resonance (SPR) peak in the ultraviolet-visible (UV-Vis) spectrum [69]. The reduction of silver salts to Ag NPs accelerated by increasing the pH of the reaction medium leads to the formation of nanoparticles. However, at a very high pH (pH > 11), there is the formation of agglomerated and unstable Ag NPs [70]. The optical band gap of Ag NPs in the basic condition is higher than in acidic and neutral conditions because of quantum size confinement [71].

Green approach synthesis of Ag NPs required a temperature lower than 100°C. The total reaction rate increased with the increasing temperature until optimum condition subsequently leading to nucleation resulting in smaller size nanoparticles. Beyond this temperature, synthesized nanoparticles have been shown to increase their size due to an increase in the fusion efficiency of metal ions that dematerialize supersaturation [72, 73].

The change in the color of plant extract during the reduction of silver salts over various times can demonstrate the formation of Ag NPs as monitored by UV-Vis spectroscopy. Similarly, Ag NPs show an SPR peak at around 450 nm. Both bathochromic and hypsochromic shifts in wavelength with reaction time have been related to different shape and size of nanoparticles formed. The shift in intensity and wavelength of the SPR peak decreased with the increase in the reaction time indicating the reduction of Ag^+ ion to Ag^0. The increase of the absorbance with the reaction time indicated an increase in the concentration of Ag NPs. Studies have shown that, after a certain time, there is no shift in the SPR peak [74, 75] indicating the stability of synthesized nanoparticles.

The concentration of silver salts determines the shape and size of product nanoparticles. Synthesis of nanoparticles can be done either by keeping salt concentration constant and adding various concentrations of extract or by preparing different concentrations of salt solution and mixed with fixed extract concentration [73]. The concentration of bioreducing agents refers to the increase in the yield of Ag NPs production having smaller sizes [76]. Higher concentration of silver salts causes formation of agglomerated and unstable higher size Ag NPs [70] (Figures 2(a) and 2(b)).

5. Characterization of Ag NPs

Ag NPs can be characterized to evaluate the functional aspects of the synthesized particles. *In situ* confirmation of its formation in colloidal solution is a preliminary analysis, followed by subsequent centrifugation/ethanol precipitation, drying, and recharacterization to evaluate different parameters. A variety of analytical techniques are used for this purpose [77–79]. The most common characterization techniques are as follows.

5.1. Characterization during Nanoparticle Formation. Characterization of Ag NPs in a colloidal solution can be performed by exploiting their optical properties that depend on the size, shape, concentration, agglomeration state, and refractive index near the surface of the nanoparticles. These properties make UV-Vis spectroscopy an important preliminary method for recognizable proof and characterization in the colloidal state. Ag NPs exhibit a UV-Vis absorption maximum in the range of 400–500 nm depending upon the particle size, and a peak in this region indicates the formation of nanoparticles due to SPR electrons on the nanoparticle surface. The concentration of reducing agents results in smaller-sized nanoparticles, which give a shift towards a lower wavelength due to the surface plasmon resonance of Ag NPs in UV-Vis spectra [76]. SPR electron excitation is characteristic of size and shape, the dielectric properties of the synthesizing medium, and the internanoparticle coupling interactions [79, 80]. Ag NPs of size 17.96 ± 0.16 nm revolved by TEM analysis were obtained when 4 : 5 ratio of 0.001 M $AgNO_3$ and aqueous extract of *Citrullus lanatus* fruit rind at the temperature of 80°C at pH 10 showed the SPR peak at 404 nm in UV-Vis spectroscopy [73].

Cyclic voltammetry utilizes the potentiodynamic electrochemical characterization of Ag NPs [81]. A significant change in the reduction potential of Ag^+ from a higher oxidation state to Ag^0 was observed during cyclic voltammetry. The cyclic voltammogram of standard 20 nm Ag NPs exhibited distinct oxidation and reduction peaks at +290 mV and +100 mV, whereas that of synthesized Ag NPs using aqueous extract of *Citrullus lanatus* fruit rind shows a distinct oxidation peak at +291 mV and no reduction peak with the size of 17.96 ± 0.16 nm [73, 82].

5.2. Characterization of Morphology and Particle Size. Transmission electron spectroscopy (TEM), scanning electron spectroscopy (SEM), atomic force microscopy (AFM), and dynamic light scattering (DLS) are characterization tools used to obtain quantitative measures of particle size, shape, and size distribution. TEM is a powerful, versatile, and high-resolution imaging technique to probe the local structure and chemistry of synthesized nanomaterials. For TEM analysis, the Ag NP sample must be ultrathin, loaded on carbon-coated copper grids by negative staining solution, and must withstand vacuum conditions. After loading, Ag NPs are allowed to dry under a mercury lamp and then exposed to a monochromatic beam of electrons to generate an image and the crystallographic structure of a sample [83, 84]. Synthesis of Ag NPs using the ethanolic root extract of *Atropa belladonna* and characterization by TEM showed the size of the nanoparticles ranged from 15 to 20 nm [6] (Figure 3).

SEM is a direct surface imaging analytical technique capable of resolving different nanoparticle sizes, size distributions, nanomaterial shapes, and surface morphology. The dried Ag NPs are coated in conductive metal using a sputter coater under ultravacuum condition. SEM uses an energetic electron beam to produce the three-dimensional structure of the particle [86]. Synthesis of Ag NPs using aqueous extract of *Musa balbisiana*, *Azadirachta indica*, and *Ocimum tenuiflorum* formed approximately spherical, triangular, and cuboidal shape nanoparticles, respectively [87]. Similarly, the synthesis of Ag NPs using an aqueous extract of *Rosa brunonii* Lindl resulted in the formation of nanoparticles with spherical shapes [88] (Figure 4).

AFM is a very effective microscopic technique for the study of the morphology of nanoparticles and is capable of reaching ultrahigh resolution based on physical scanning in either liquid or gas medium. The instrument generates a topographical map of the Ag NPs based on the different forces (magnetic, electrostatic, and interatomic forces) between the probe and the surface of the nanoparticles [86]. Kumar et al. synthesized the Ag NPs using aqueous extract of *Adansonia digitata* fruit pulp with 25–57 nm size and spherical and polydispersed morphology confirmed by AFM [90].

DLS is utilized for deciding particle size and distribution by measuring the rotational and translational diffusion coefficients of the particle. It measures the size of Brownian particles in colloidal suspensions. At the point when a monochromatic light directs onto a solution of Ag NPs, a

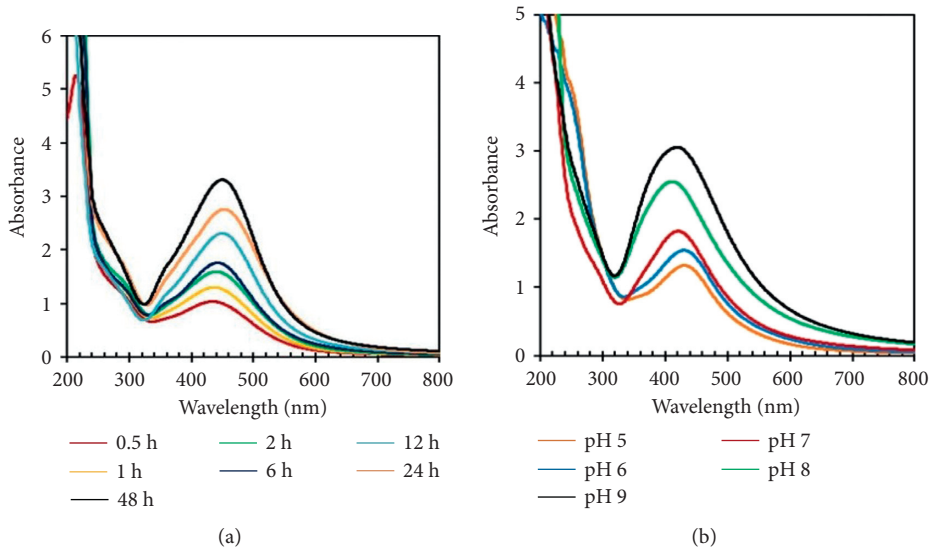

Figure 2: (a) Time-dependent absorption spectra of the reaction mixtures consisting of $AgNO_3$ and *Piper chaba* extract at 60°C and pH = 7 [59] (open access and reprinted under CC BY 4.0). (b) pH-dependent absorption spectra of the reaction mixtures of AgNO3 and *Piper chaba* extract after the reaction for 1 h at 60°C [59] (open access and reprinted under CC BY 4.0).

Doppler shift occurs when the light hits the moving particles, along with changing the wavelength of the incoming beam of light by a value related to particle size and distribution using the Stokes–Einstein relationship [91, 92]. Synthesis of Ag NPs using aqueous extract of *Chamaemelum nobile* and DLS analysis confirmed the 39–78.5 nm size at optimum condition [93].

5.3. Characterization of Surface Charge and Stability. The net effective electric charge at the double layer boundary is the zeta potential that gives an idea about the electropotential status of the Ag NPs in a dispersed medium. Laser Doppler electrophoresis is the most common and accepted method for surface charge characterization and stability of nanoparticles because of better resolution and more reliable results. The motion of nanoparticles depends on the surface charge, and the movement of nanoparticles is due to the Brownian motion and electrostatic forces under the impacts of applied electric fields. The high negative potential value of Ag NPs underpins long-term stability, high surface charge, good colloidal nature, and high dispersity of nanoparticles due to negative-negative repulsion [94–96]. *Annona squamosa* leaf was used to synthesize Ag NPs having a zeta potential of 37 mV [97]. *Cynara scolymus* leaf extract mediated Ag NPs with zeta potential values of -32.3 ± 0.8 mV were reported indicating negatively charged and stable nanoparticles [8]; the zeta potential value higher than +30 mV or lower than −30 mV is considered to be very stable in the dispersion medium.

5.4. Characterization of Crystallinity. X-ray diffraction (XRD) is a nondestructive analytical technique to determine the crystallographic parameters of the nanoparticles. Examination of nanoparticles relies upon the formation of diffraction patterns which depends on the size and crystal structure. The 2θ, d-spacing values, lattice constant, and cell volume confirm the crystallinity of green synthesized nanoparticles and crystallite size. Average particle crystallite sizes are determined from the XRD spectra using the Debye–Scherrer equation [98, 99]. Broad XRD peaks indicate the presence of smaller size of Ag NPs and the crystallinity of Ag NPs. Ag NPs synthesized using ethanolic *Santalum album* fruit extract and XRD analysis showed FCC crystal structure, and the average crystalline size is estimated to be 20 nm [98].

6. Challenges on the Plant-Mediated Synthesis of Ag NPs

High reproducibility is a demanding concern in the synthesis of nanoparticles. However, environmental factors (seasonal variation, geographic variation, water tension, lack of light access, attacks of herbivores and parasites, pH of the soil, etc.), unintentional and intentional factors (pollution and usage of herbicides and pesticides), and anthropogenic behavior may affect the formation of bioreducing secondary metabolites. In addition to this, powerful chemical reduction agents such as alkali metal borohydrides are favored compared to the weak reducing agents from plants' secondary metabolites. It is because plant extracts serve as weak reducing agents, tend to nucleate particles far slower, and produce large nanoparticles and polydisperse products that may need postprocessing [100, 101], while stronger chemical reducing agents generate tiny nanoparticles [102]. Stronger secondary metabolites from the plant as reducing agents need to be identified, or new strategies need to be developed to increase the ability of existing green agents and to eliminate toxic reducing agents. Ligands are frequently used to passivate the surfaces of the nanoparticles, which serve to limit growth, stabilize against aggregation, and provide the

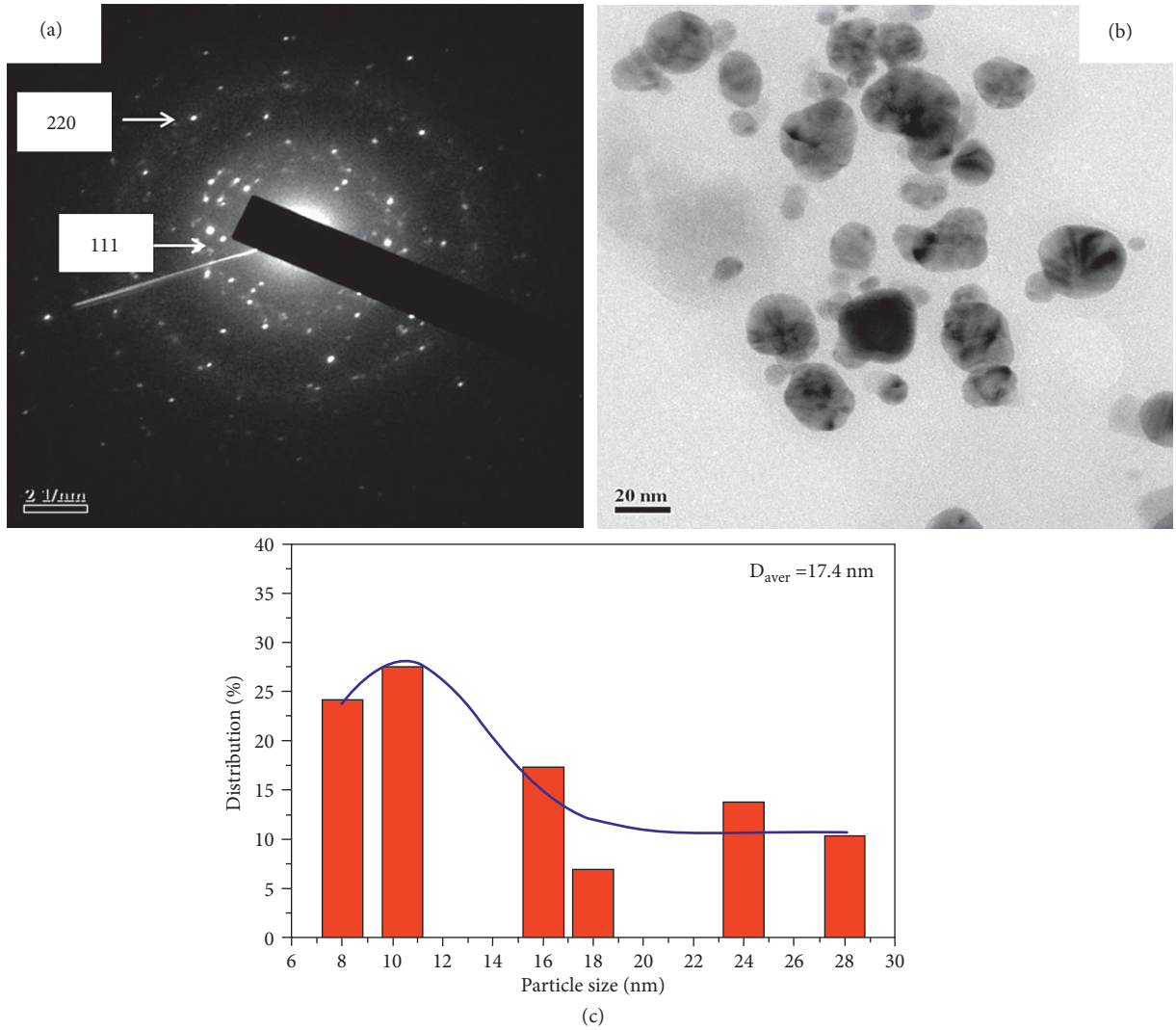

Figure 3: TEM micrograph of the synthesized Ag NPs. (a) SAED pattern of synthesized Ag NPs. (b) Analysis of the morphology of Ag NPs. (c) Histogram showing the size distribution of Ag NPs [85] (open access and reprinted under CC BY 4.0).

ability of functionalization. Secondary metabolites from natural products give a range of renewable options of stabilizing/capping agents that can be of low cost and manufactured locally; however, the polydispersity of the products is again a major issue with such alternative ligands. Usually, polydispersity involves postprocessing, which increases waste but can also restrict clinical applications if the physicochemical properties differ across lots. In this regard, the use of glutathione, a natural and ubiquitous tripeptide, is especially attractive in the synthesis of discrete molecular nanoparticles [103].

7. Application of Green Synthesized Ag NPs

7.1. Antibacterial Activity. Silver ions, Ag NPs, and synthesized nanoparticles doped with other compounds induce toxicity towards microorganisms [104, 105]. The synthesized Ag NPs demonstrate promising antimicrobial activities against both Gram-negative and Gram-positive bacteria [106]. Ag NPs show antibacterial properties by disabling the respiratory chain, or disrupting the cell membrane and causing rupture of cellular contents, or attaching to a functional group of proteins causing protein denaturation, or blocking genetic material replication [107].

Ag NPs synthesized using *Cestrum nocturnum* extracts have been shown to produce a spherical shape with 20 nm size. The MIC value of synthesized nanoparticles against *Citrobacter*, *E. faecalis*, *S. typhi*, *E. coli, P. vulgaris*, and *V. cholera* was found to be 16 μg/ml, 4 μg/ml, 16 μg/ml, 8 μg/ml, 8 μg/ml, and 16 μg/ml, respectively. The enhanced antibacterial activity was attributed to the presence of bioactive compounds on the surface of nanoparticles as stabilizing agents/capping agents [108].

In *Citrus limetta* peel extract mediated Ag NPs, 107 μg/ml concentration showed the highest zone of inhibition in *E. coli* among five test bacterial strains, while MIC, MBC, and IC_{50} values of Ag NPs in *E. coli* are 4.75, 13.38, and 4.28 μg/ml, respectively [109]. *Moringa oleifera* flower extract used to synthesize Ag NPs was stable for six months and have more toxicity towards *S. aureus* with a zone of

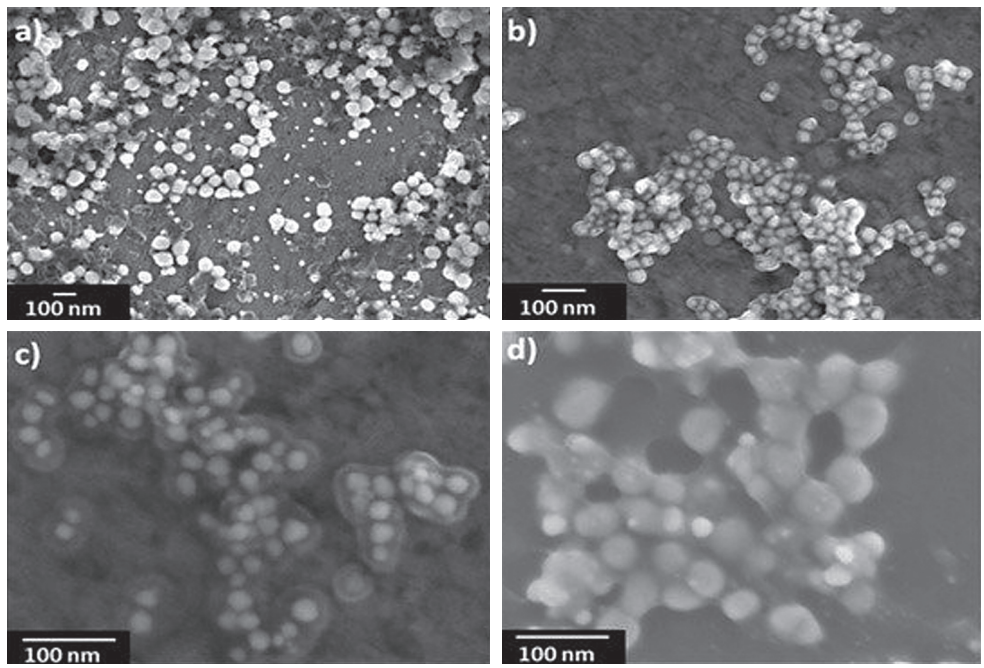

Figure 4: SEM images at different magnifications: (a) 50,000x, (b) 100,000x, (c) 200,000x, and (d) 220,000x [89] (open access and reprinted under CC BY 4.0).

Table 1: Morphology of Ag NPs and their antibacterial properties.

Size by TEM with morphology	Antibacterial activity			References
	Bacterial strains	ZOI (mm)	MIC	
TEM 10–30 nm Spherical in shape	*B. cereus*	16	5.2 μg/ml	[118]
	S. aureus	12	2.6 μg/ml	
	E. coli	17	2.0 μg/ml	
TEM 40–50 nm SEM 50–60 nm Spherical in shape	*E. coli*	25	3.9 μg/ml	[119]
	P. aeruginosa	27	1.95 μg/ml	
	S. aureus	24	3.9 μg/ml	
	B. subtilis	24	15.62 μg/ml	
TEM 25 nm average Spherical in shape	*F. branchiophilum*	15	3.12 μg/ml	[120]
	A. hydrophila	14	25 μg/ml	
	P. fluorescence	12	50 μg/ml	
TEM 23.7 nm average Spherical in shape	*B. subtilis* (local)	12	6.8 μg/ml	[66]
	S. aureus	16	5.1 μg/ml	
	P. aeruginosa	20	1.70 μg/ml	
	P. aeruginosa (local)	18	1.70 μg/ml	
	E. coli	17	3.4 μg/ml	
TEM 15–20 nm Spherical in shape	*S. aureus*	14.93 ± 0.57	60 μM	[6]
	E. coli	18.13 ± 0.47	60 μM	

inhibition of 29 mm as compared to *K. pneumoniae* with 17 mm [110]. Secondary metabolites present in *Mentha aquatica* leaf extracts act as a bioreducing agent for silver nitrate salt via ultrasound-assisted and hydrothermal methods. In *S. aureus*, the MIC values of synthesized Ag NPs via ultrasound-assisted route are significantly lower than the ones produced via hydrothermal route among four test bacterial strains [111]. Ag NPs synthesized using the extract of clove buds yielded particles with an average size of 9.42 nm, which was confirmed by TEM, and showed good marine antibacterial activity [112]. *Curcuma longa* L. was used to synthesize Ag NPs, and 35 μg concentration of the nanoparticles showed good antibacterial activity against *P. aeruginosa* and *S. aureus* with an MIC value of 1.25 μl [113]. Ag NPs synthesized at neutral pH using *Ziziphus joazeiro* leaf extract showed good antibacterial activity against both Gram-positive and Gram-negative bacteria. In neutral pH, size control is more pronounced than in both acidic and basic pH. The Ag NPs synthesized under basic conditions have negligible antibacterial activity against *S. aureus* but superior activity against *E. coli*, while the ones synthesized in acidic conditions have oppositive activity

Table 2: Morphology of green synthesized Ag NPs and their antiviral activity on different viral strains.

Phytoconstituents	Size by TEM/SEM with morphology	Viral strain	Antiviral activity (IC_{50}/MNTD/$TCID_{50}$/ml)	Reference
Alkaloids, terpenoids, flavonoids, glycosides, phenols, and tannins	TEM 27.89 nm Spherical in shape	HSV-1 HAV-10 CoxB4	IC_{50} 36.36 μg/ml 11.71 μg/ml 12.24 μg/ml	[127]
Polyols, flavonoids, polyphenols, and terpenoids	SEM average size 70–95 nm	Chikungunya	MNTD: 31.25 μg/mL	[4]
Polyphenols	SEM average size 100 nm Spherical in shape	Dengue (DEN-2)	$TCID_{50}$/ml Viral titer 3.2 log10 at 20 μl/ml Ag NPs	[128]
Lignocellulose	TEM 3–10 nm Narrow in shape	Chikungunya	IC_{50}: 11.73 μg/ml	[129]
—	SEM average size 42 nm Spherical in shape	H7N3 influenza virus	IC_{50}: 101 μg/ml (during viral infection) and 125 μg/ml (after viral infection)	[130]

Table 3: Morphology of plant-mediated synthesized Ag NPs and their antifungal activity.

Size by TEM with morphology	Operational condition	Fungal strains	ZOI	IC_{50}/MIC_{50}/MFC/MIC	Reference
TEM 18 nm average size with spherical shape	An aqueous solution of 0.001 N $AgNO_3$ was mixed with *Citrus limetta* peel extract in a 5 : 1 ratio and continuously stirred	*C. albicans* *C. glabrata* *C. parapsilosis* *C. tropicalis*	15 ± 0.75 mm 14 ± 0.70 mm 14 ± 0.70 mm 14 ± 0.70 mm	4.75 μg/mL 5.94 μg/mL 4.75 μg/mL 5.94 μg/mL IC_{50}	[109]
TEM 13 nm average size with spherical shape	1 : 4 ratio of *Ligustrum lucidum* leaf extract and 1 mM $AgNO_3$ heated at 80°C	*S. turcica*	3.7 cm	170.20 μg/mL IC_{50}	[139]
TEM 10–32 nm with spherical shape	1 : 9 ratio of *Amaranthus retroflexus* leaf extract and 1 mM $AgNO_3$ solution allowed to stand overnight	*M. phaseolina* *A. alternata* *F. oxysporum*	— — —	159.80 ± 14.49 μg/mL 337.09 ± 19.72 μg/mL 328.05 ± 13.29 μg/mL MIC_{50}	[140]
TEM 20–40 nm size with spherical shape	1 : 9 ratio of *Gelidium corneum* extract and 1 mM $AgNO_3$ exposed to a controlled temperature for 30 minutes	*C. albicans*	—	2.04 μg/mL (MFC) 0.51 μg/mL (MIC)	[141]
TEM 5–10 nm size with spherical shape	1 : 9 ratio of *Selaginella bryopteris* leaf extract and 1 mM $AgNO_3$ with continuous stirring for 10 min followed by sonication at 80°C	*A. niger*	1 mm	10 mg/mL	[142]

Table 4: Morphology of green synthesized Ag NPs and their anti-inflammatory activity on different inflammation models.

Size by TEM/SEM with morphology	Inflammation model	%inhibition/IC_{50}/binding constant	Reference
SEM 32–38 nm size with spherical shape	BSA protein	Binding constant (2.01 ± 0.06) × 10–4	[152]
TEM 15–20 nm size with spherical shape	BSA protein	IC_{50}: 84 μM	[6]
—	Protein inhibitory activity Albumin denaturation Membrane stabilization	89.17 + 1.4% 84.64 + 1.4% 84.18 + 1.4%	[153]
TEM 25 nm average size with spherical shape	HaCaT cells	IL-1α-55% IL-1β-69% IL-6-68%	[154]
TEM 20–80 nm size with spherical shape	HaCaT cells	IL-1α-49% IL-1β-92% IL-6-74%	[155]

Table 5: Morphology of green synthesized Ag NPs and their antidiabetic activity.

Size by TEM/SEM with morphology	Operational condition	Antidiabetic activity		Reference
		Enzyme	IC_{50}	
SEM 10–25 nm with spherical shape	1 : 10 ratio of *Pisum sativum* L. outer peel extract and 1 mM $AgNO_3$ stirred continuously for 24 hours	α-Glucosidase	2.10 μg/mL	[94]
TEM 5–50 nm with rod, spherical, and triangular shape	1 : 2 ratio of different concentrations of $AgNO_3$ and *Cleome viscose* whole plant at room temperature	α-Amylase	21.92 ± 1.74 μg/mL	[167]
		α-Glucosidase	21.76 ± 1.91 μg/mL	
TEM mean diameter of 3.45 ± 0.16 nm with monodispersed and spherical shape	40 : 1 ratio of 1 mM $AgNO_3$ and aqueous flower extract of *Dregea volubilis* at 121°C and 15°psi pressure for 20 minutes	α-Amylase	10.62 ± 0.22 μg/mL	[168]
		α-Glucosidase	6.49 ± 0.03 μg/mL	
TEM 5–15 nm with polydispersed and spherical shape	1 : 99 ratio of 1 mM $AgNO_3$ and flower aqueous extract of *Bauhinia variegate* incubated in dark at room temperature for 1 hour	α-Amylase	38 μg/mL	[169]
SEM 50 nm with polydispersed shape	1 : 19 ratio of *Xylocarpus granatum* bark aqueous extract and 10 mM $AgNO_3$ at room temperature for 6 hours	α-Amylase	0.19 mg/mL	[170]
		α-Glucosidase	0.13 mg/mL	

[114]. Bioreduced Ag NPs showed higher antibacterial activity than the crude extract alone [115, 116]. Ag NPs synthesized using the extract of *Ziziphora clinopodioides* (pH of 8, 4 mM of $AgNO_3$, and time of 2.5 hours) resulted in spherical nanoparticles with an average size of 25–50 nm. The synthesized Ag NPs showed excellent antibacterial properties in both Gram-positive *S. aureus* and Gram-negative *E. coli* [117]. Table 1 shows the morphology of Ag NPs and their antibacterial property against Gram-positive and Gram-negative bacteria.

7.2. Antiviral Activity. Various viruses are likely to erupt highly infectious diseases that increase day by day which threatens human health [121]. The surface chemistry of Ag NPs and their size determine the antiviral activity. The possible mode of action is to hamper the binding with the extracellular matrix inhibiting interaction towards outer cell receptors or with the genetic material [122]. The broad spectrum of Ag NPs is efficient and effective against viral strains and the risk of resistance by mutation [123]. Ag NPs with size ≤10 nm effectively bind to sulfur-bearing residues in gp120 glycoprotein knobs in the outer surface of the human immune deficiency virus (HIV-1) that hinders the binding with the host cell and thus inhibits its activity [124].

Quasi-Ag NPs synthesized from an aqueous extract of *Panax ginseng* roots are virucidal against the influenza A virus (strain A/PR/8). Slight anti-influenza effects have been observed with 0.005, 0.01, and 0.15 M concentrations of Ag NPs with inhibitory rates of 5.31%, 4.18%, and 5.97%, respectively. However, the virucidal inhibitory activity has been reported to have significantly increased to 7.10% and 15.12% at concentrations of 0.02 and 0.25 M, respectively [125]. Synthesis of Ag NPs from the aqueous leaf extracts of mangrove *Rhizophora lamarckii* resulting polydispersed spherical nanoparticles, with particle size ranging from 12 to 28 nm by TEM analysis, exhibited potent HIV-1 reverse transcriptase inhibitor activity with an IC_{50} value of 0.4 μg/mL [126]. Table 2 shows the morphology of green synthesized Ag NPs and their antiviral activity on various viral strains.

7.3. Antifungal Activity. Fungal infections, particularly nosocomial fungal infections, are a major health risk [131] against which biomediated Ag NPs can be employed. Antibacterial activities of Ag NPs are well established, while antifungal activities have still not been thoroughly examined. Ag NPs are commonly known for strong antimicrobial activity even at very low concentrations [132]. Ag NPs showing antifungal properties lead to the destruction of either cell wall or cell membrane and deposition around the cell leading to damage or degeneration of organelles (chromatin, ribosomes, and mitochondria) [133]. Several experiments have demonstrated that Ag NPs exhibit strong antifungal properties against *Colletotrichum coccodes*, *Monilinia* species [134], and *Candida* species [135]. Ag NPs synthesized using the methanolic leaf extract of *Atalantia monophylla* (2 mM of $AgNO_3$ and time of 15 minutes) result in spherical Ag NPs (average size of 35 nm) that exhibit better antifungal activity against *Candida albicans* [136].

Teucrium polium L. flower extract was used in the synthesis of spherical Ag NPs and used against *Fusarium oxysporum*, a plant pathogenic fungus. The concentration of Ag NPs from 50 to 1500 ppm resulted in a decrease in the colony diameter and mean growth inhibition percentage, and colony formation was quenched at higher concentrations of the nanoparticles. However, the concentration of 1500 ppm Ag NPs did not fully inhibit colony formation [137]. The Ag NPs synthesized by *Andrographis paniculata* extract have FCC crystalline structure with an average size of 24.5 nm and spherical shape and have effective antifungal activity at 50 μg/mL. It was concluded that the presence of

Table 6: Operational condition during synthesis of Ag NPs and their anticancer activity on different cell lines.

Size by TEM/SEM with morphology	Operational condition	Anticancer activity		
		Cell line	IC_{50} (μg/mL)	References
TEM 33 nm average size with spherical shape	9 : 1 ratio of 0.1 M $AgNO_3$ and *Nepeta deflersiana* extract incubated for 24 hours and then continuously stirred at 90°C	HeLa	5	[179]
SEM 30–50 nm with spherical shapes	9 : 1 ratio of 1 mM $AgNO_3$ and *Cucumis prophetarum* leaf extract followed by heating at 80°C for 3 hours with constant stirring	A549	105.8	[79]
		MDA-MB-231	81.1	
		HepG2	94.2	
		MCF-7	65.6	
TEM 6.7 nm average size with spherical shape	4 : 1 ratio of 1 mM $AgNO_3$ and *Abelmoschus esculentus* pulp extract at room temperature with continuous stirring for 9 hours	Jurkat cells	16.15	[180]
TEM 40–80 nm with spherical shape	3 : 10 ratio of *Salacia chinensis* bark extract and 1 mM $AgNO_3$ heated at 65°C for 15 minutes	HepG2	6.31	[181]
		L-132	4.002	
		MIA-Pa-Ca-2	5.22	
		MDA-MB-231	8.452	
		KB cells	14.37	
		PC-3	7.46	
		HeLa	6.55	
SEM 15.6 nm average size with spherical shape	1 : 1 ratio of 6 mM $AgNO_3$ and *Punica granatum* fruit extract at 37–40°C under stirring in dark for 24 hours and pH 8	BT-20	37	[182]
		MCF-7	17	

Table 7: Morphology of green synthesized Ag NPs and their pesticide activity on different species.

Phytoconstituent present	TEM with morphology	Nanopesticide activity			Reference
		Test species	Time of exposure	LC_{50}	
Alkaloids, acids, and terpenoids	TEM 20 nm with polyhedral shape	*Culex quinquefasciatus*	72 hours	1.26 ppm	[190]
		Anopheles stephensi	72 hours	1.33 ppm	
Tannins, phenols, flavonoids, saponin, and terpenoids	TEM 5–25 nm with spherical, hexagonal, triangular, and polyhedral shape	*Aedes aegypti*	24 hours	4.63 mg/L	[191]
		Anopheles stephensi	24 hours	4.04 mg/L	
		Culex quinquefasciatus	24 hours	3.52 mg/L	
Flavonoids, triterpenoids, and polyphenols	TEM 18–35 nm with spherical shape	*Anopheles subpictus*	24 hours	31.56 μg/mL	[192]
		Aedes albopictus	24 hours	35.21 μg/mL	
		Culex tritaeniorhynchus	24 hours	38.08 μg/mL	
Flavonoids, triterpenoids, and polyphenols	TEM ~6.48 ± 1.2 to 8.13 ± 0.18 nm with spherical shape	*Aedes aegypti*	24 hours	4.43 μg/mL	[193]
Flavonoids, terpenoids, steroids, and alkaloids	TEM 32 nm average size with spherical, triangular, truncated triangular, and decahedral shape	*Anopheles stephensi*	24 hours	22.44 μg/mL	[194]
		Aedes aegypti	24 hours	25.77 μg/mL	
		Culex quinquefasciatus	24 hours	27.83 μg/mL	

bioactive compounds as stabilizing agents/capping agents on the surface of Ag NPs enhanced its antifungal activity [138]. Table 3 shows the morphology of plant-mediated synthesized Ag NPs and their antifungal activity on different fungal strains.

7.4. Anti-Inflammatory Properties. Researchers have already demonstrated that nanoparticles tend to have anti-inflammatory properties, where Ag NPs have been involved in decreasing inflammation in peritoneal adhesions with no noticeable toxic effects [143]. Inflammation although is a

Table 8: Morphology of green synthesized Ag NPs and their catalytic activity on different substrates.

Size by TEM/SEM with morphology	Catalytic activity				Reference
	Substrate	Type of reaction	Time (min)	Yield (%)	
TEM 10–50 nm with spherical shape	4-Nitrophenol	Reduction	20	88.80	[11]
SEM 20–60 nm with spherical shape	1-Phenylethanol	Oxidation	480	62	[200]
Spherical in shape with narrow size	4-Methyl phenyl cyanide	Hydration	60	95	[201]
TEM 2.76 nm with spherical shape	Benzaldehyde, morpholine, phenylacetylene	A^3 coupling	480	95	[202]
TEM 10–35 nm with spherical and oval shape	3-Amino indazoles, 2-methoxy benzaldehyde, and ethynyl benzene	A^3 coupling	60	96	[203]

significant form of defense in the human body [144], excessive inflammation, may cause multiple diseases including cancer, arthritis, and neurological disorders [145] distinguished by the development of proinflammatory cytokines and by the stimulation of immune system cells. The pathways of the nuclear factor-kappa B (NF-κB) play a crucial role in the inflammation cycle, raising the rates of cytokines and inflammatory mediators such as nitric oxide, prostaglandin E2, inducible nitric oxide synthase, and lipopolysaccharides-2 [146]. The intracellular blocking of inflammatory pathways and downregulating proinflammatory cytokines could be the potential mechanism of Ag NPs anti-inflammatory properties [147]. Green synthesized Ag NPs suppressed LPS-mediated induction of protein levels through NF-κB signaling via the p38 MAPK pathway and can be used as an effective agent in anti-inflammation [148].

Avicennia marina ethanolic extract synthesized Ag NPs exhibit an effective inhibition of heat-induced albumin denaturation of 68.92% and 72.1%, respectively [149]. Belle Ebanda Kedi et al. studied the ability of the *Selaginella myosurus* extract mediated Ag NPs to inhibit thermally induced egg albumin denaturation by arthritic reactions and development of tissue damage during the inflammation process indicating their ability to control protein denaturation [150]. The anti-inflammatory potential of synthesized Ag NPs using *Atropa acuminata* aqueous leaf extract was shown by albumin denaturation and antiproteinase activity with IC_{50} values 12.98 and 18.401 μg/mL, respectively, which is lesser than the standard anti-inflammatory drug, diclofenac sodium salt. This is because inhibiting the production of autoantigens that reduce the denaturation of albumin and retard the production of neutrophils leads to prevent tissue damage. It is evident that green synthesized Ag NPs exhibited strong anti-inflammatory activities and could be used as potential anti-inflammatory drugs [151]. Table 4 shows the morphology of green synthesized Ag NPs and their anti-inflammatory activity on different inflammation models.

7.5. Antidiabetic Activity. Diabetes mellitus (DM) is a group of metabolic chronic disorders characterized by postprandial hyperglycemia resulting from anomalous insulin secretion, insulin action, or both and disturbances of carbohydrate, lipid, and protein metabolism, creating a high risk of premature mortality, bringing immense financial pressure on public health systems and national economies. It is estimated that 463 million people have diabetes, and this figure is expected to hit 578 million by 2030 and 700 million by 2045 [156]. Diabetes may lead to long-term damage, dysfunction, and failure of various organs, especially the eyes, kidneys, nerves, heart, blood vessels, and so on [157–159]. α-Amylase and α-glucosidase are major hydrolytic enzymes involved in diabetes and responsible for the hydrolysis of carbohydrates in the luminal digestive tract. These two enzymes act at the same time, and the α-glucosidase activity is the rate-determining step in carbohydrate hydrolysis [160]. Inhibition of α-amylase and α-glucosidase enzymes leads to a decrease in blood glucose level in the body [161]. Acarbose, voglibose, and miglitol are commercially available drugs to inhibit these digestive enzymes in diabetic patients, but adverse effects such as meteorism, flatulence, and diarrhea are frequently observed [162]. This warrants the search for safe and effective treatment modalities that have lesser side effects than the currently available drugs; the green synthesized Ag NPs modality is one of them. Ag NPs synthesized from aqueous leaf extract of *Lonicera japonica* showed potent inhibition against carbohydrate digestive enzymes such as α-glucosidase and α-amylase with IC_{50} values of 37.86 and 54.56 μg/mL, respectively. Besides, kinetic studies have revealed Ag NPs to be reversible noncompetitive inhibitors with Ki values of 25.9 and 24.6 μg for α-amylase and α-glucosidase, respectively [163].

Punica granatum leaf extract used to synthesize Ag NPs with an average size of 20–45 nm with spherical shape showed effective inhibition against α-amylase and α-glucosidase with IC_{50} values of 65.2 and 53.8 μg/mL, respectively. Synthesized nanoparticles have higher hydrolytic enzyme inhibition potential than plant extract and slightly lower than standard drug acarbose [164]. Ag NPs synthesized from the flower aqueous extract of *Momordica charantia* are spherical with 22.5 nm by SEM analysis. The nanoparticles showed a decrease in blood glucose at a dose of 200 mg/kg in STZ-induced diabetic rats, and similarly, the regeneration of necrotic beta cells was especially pronounced at that dose [165]. Outer peel extract of the fruit *Ananas comosus* was used to synthesize Ag NPs exhibiting promising α-glucosidase inhibition potential in a dose-dependent manner. 100% inhibition of α-glucosidase was

Table 9: Morphology of green synthesized Ag NPs and their dye degradation activity.

Phytoconstituent present	TEM with morphology	Dye degradation			References
		Dye used	Reaction time (min)	Rate constant (min^{-1})	
Phenols and flavonoids	TEM 19.06 nm average size with spherical shape	Methyl orange	9	0.9906	[216]
		Methylene blue	11	0.2385	
Phenols and flavonoids	TEM 10–25 nm with spherical shape	Congo red	9	0.6	[217]
Polyphenol and flavonoids	TEM 16 nm average size with spherical shape	Brilliant blue	20	0.2097	[210]
		Tartrazine	40	0.0076	
		Carmoisine	15	0.0496	
Phenol	TEM 62.51 nm with spherical shape	Methylene blue	18	0.1448	[218]
Polyphenol	TEM 7 nm with spherical size	Methylene blue	0.83	5.18	[202]
		Rhodamine B	1	3.44	

observed at 0.063 μg/mL concentration of synthesized nanoparticles [166]. Table 5 shows the morphology of Ag NPs, operational condition, and antidiabetic activity by inhibitory activity on two major enzymes, α-glucosidase and α-amylase.

7.6. Anticancer Activity. Cancer is a life-threatening disease that emerges from the deterioration of normal cells into tumor cells in a multistage process due to genetic factors and physical, chemical, and biological carcinogens [171]. Distinctive types of cancers are known; among them, lung, colorectal, stomach, liver, and breast cancers are more common according to WHO. Green synthesized Ag NPs have proven to have antiproliferative and apoptosis-inducing properties and are thus used as anticancer agents. Ag NPs enter the mitochondria by endocytosis, which leads to the generation of ROS, and alteration of the adenosine triphosphate synthesis. Ag NPs are toxic to cancerous cells and lead to DNA damage, oxidative stress, induction of apoptosis, or mitochondrial damage. Ag NPs alter the function of the vascular permeability factor and play a major role in the angiogenesis within cancer. Phytochemically reduced Ag NPs are used for the treatment of cancer due to their safety, low toxicity, and cheaper cost [172–174].

The unique physicochemical property of green synthesized Ag NPs and their entrance into the cells can interact with biomolecules inside the cells. Spherical Ag NPs with an average size of 43.5 nm synthesized using *Delonix regia* leaf aqueous extract behave as anticancer agents. *In vitro* examination on A549 and SiHa cell line by MTT assay and Ag NPs have shown to have potent antiproliferative activity. Half-maximal inhibitory concentration (IC_{50}) gives the 50% inhibition of biological or biochemical function. The green synthesized nanoparticles exhibited an IC_{50} value of 14.96 and 15.96 μg/mL after 48 hours for A549 and SiHa, respectively [175].

Spherical and triangular Ag NPs with sizes varying from 24 to 80 nm synthesized using *Commelina nudiflora* L. have shown potent cytotoxicity against HCT-116 colon cancer cells. The cytotoxicity increased by the increase in concentrations with an IC_{50} value of 100 μg/ml in 24 hours of exposure. The use of Ag NPs has shown 90% cell death at 250 μg/ml concentration, the treated cell line underwent membrane blebbing, and morphological change led to induced apoptosis [176]. *Cornus officinalis* used to synthesize Ag NPs having well-dispersed and quasispherical shape with an average size of 11.7 nm showed cytotoxicity against PC-3 and HepG2 cell lines with LC_{50} values of 25.54 and 21.46 μg/mL in 48 hours [177]. *Caesalpinia pulcherrima* used to synthesize Ag NPs showed *in vitro* cytotoxicity against HCT-116 cells having an IC_{50} value of 3.8 μg/mL [178]. Table 6 shows operational conditions during the synthesis of Ag NPs and their anticancer activity on different cell lines.

7.7. Nanopesticide Activity. Pesticides have been deeming as one of the world's main leading factors to environmental pollution. The intended applications of these chemicals have proven to be toxic to pests and disease vectors, with over 1000 active ingredients sold as insecticides, herbicides, and fungicides [183]. Although pesticides have primarily improved the quality of human life and the prevention of infectious diseases, however, pesticide toxicity is believed to be related to a variety of health problems such as Parkinson's disease [184], endocrine destruction [185], cardiovascular diseases, cancer, reproductive disorders [186], and so on. Therefore, this review is based on nanopesticides due to their nature of being less toxic and ecofriendly. Ag NPs act as an effective pest management product and are nontoxic, stable, and innovative pest control tool. Researchers have reported the potential application of UV-irradiated Ag NPs in pest biocontrollers, such as mosquito larvae. *Delphinium denudatum* aqueous root extract is used in the synthesis of polydispersed and spherical shape Ag NPs. These nanoparticles showed potent larvicidal activity against the dengue vector *Aedes aegypti* second-instar larvae with an LC_{50} value of 9.6 ppm in 48 hours of exposure. *Aedes aegypti* second-instar larvae can no longer survive at higher concentrations, and no significant difference was found between the time of exposure [187]. Similarly, the green synthesized nanoparticles showed lower LC_{50} value as compared to $AgNO_3$ on

Table 10: Morphology of Ag NPs, their metal sensing activity, and their detection limit.

Phytoconstituents	TEM with morphology	Metal sensing activity				Reference
		Metal ions	Operational condition	Concentration range	Detection limit	
Flavonoids, phenols, sugars, and P-substituted aryl compounds	TEM 15 nm with spherical shape	Fe^{+3}	Ag NPs addition of various metal ions (Al^{3+}, Fe^{3+}, Co^{2+}, Pb^{2+}, Cu^{2+}, Ni^{2+}, Zn^{2+}, Cr^{3+}, Mn^{2+}, and Cd^{2+}) showed selective detection towards Fe^{3+} only	30–150 μm	4.5 μm	[227]
—	TEM 15–20 nm with spherical shape	Cu^{2+}	Rhodamine 6G dye fixed on the surface of Ag NPs to which 1 mL of test solution of various metal ions (Cu^{2+}, Mg^{2+}, K^{+}, Mn^{2+}, Fe^{3+}, Zn^{2+}, Co^{2+}, and Ba^{2+}) was added	10^{-6}–10^{-13} mol/L	10^{-13} mol/L	[228]
Flavonoids, tannins, phenol, saponins, and glycosides	TEM 25 ± 5 nm average size with spherical shape	Hg^{2+}	10^{-3} M solution of Li^{+}, Al^{3+}, Cr^{3+}, Mn^{2+}, Fe^{3+}, Co^{2+}, Ni^{2+}, Cu^{2+}, Hg^{2+}, Cd^{2+}, and Pb^{2+} added to equal amount of Ag NPs	10^{-4}–10^{-6} M	10^{-3} M	[229]
Polyphenols and flavonoids	TEM 19.7 nm with spherical shape	Cd^{2+}	Cd^{2+}, Ni^{2+}, Cu^{2+}, Zn^{2+}, Cr^{3+}, Fe^{2+}, Pb^{2+}, Co^{2+}, and Hg^{2+} solution added to Ag NPs which showed a selective detection towards Cd^{2+} only with the highest response at a pH of 6	10–90 μM	70 μM	[230]
Citric acid	TEM 10.82 nm with spherical shape	Cr^{3+}	Ag NPs tested by adding different metal ions (Cu^{2+}, Zn^{2+}, Cd^{2+}, Hg^{2+}, Pb^{2+}, Co^{2+}, and Cr^{3+}) and color change observed only for Cr^{3+} at an optimum pH of 8	10–90 μM	0.804 μM	[231]

Table 11: Morphology of Ag NPs and their aquatic toxicity in different species.

Size by TEM with morphology	Toxicity in aquatic species			Reference
	Species	LC_{50}/LC	Effects	
—	*Poecilia reticulata*	3 μg/mL	Gill stimulation and increased mucus secretion	[236]
	Ceriodaphnia cornuta	35 μg/mL	Aggregates in gastrointestinal tract damage in the organs	
TEM 10–50 nm with spherical and polydispersed shape	*Ceriodaphnia cornuta*	23.5 μg/ml	Bioaccumulation of nanoparticles in the internal gut region and blackening of the intestine lead to rupture of the abdomen	[237]
	Paramecium sp.	15.5 μg/mL	Morphological deformities	
	Poecilia reticulata	38.3 μg/mL	Congestion in the hepatic parenchyma	
—	*Danio rerio*	3×10^{7} mL^{-1}	Damage in the gill cells	[238]
TEM 10 nm average size with spherical shape	*Danio rerio*	80 μg/ml	Disorders in organogenesis throughout the development	[239]
TEM 76.94 ± 36.82 nm with spherical and quasispherical shape	*Daphnia magna*	1.86 ± 0.12 μg/L	Generation of ROS and oxidative stress and cause negative effects	[240]
TEM 5–50 nm with spherical shape	*Danio rerio*	142.2 μg/L	Oxidative stress and immunotoxicity	[241]
TEM 50 nm average size with spherical shape	*Labeo rohita*	25 μg/L	Oxidative stress and histopathological alterations in the gills, liver, and kidney	[242]

the third larvae stage of *Culex pipiens* and *Musca domestica* [188]. The green synthesized Ag NPs from the aqueous aerial extract of *Ammannia baccifera* showed significant toxic effects against the larvae of *Anopheles subpictus* and *Culex quinquefasciatus* with LC_{50} values of 29.54 ppm and 22.32 ppm, respectively [189]. Table 7 shows the morphology

of green synthesized Ag NPs and their pesticide activity on different species.

7.8. Catalytic Activity. Catalysis has become an ambitious field in nanoscience and emerging applications because of its unique properties such as high surface-to-volume ratio, compositional tenability, and ease of recovery [195]. Ag NPs can oxidize and then reduce metal back to zero under mild conditions, allowing Ag NPs to behave as strong catalysts in both reductive and oxidative processes due to the particular location of Ag^+/Ag^0 couple redox potential [196]. Ag NPs also have a fascinating optical feature, the localized surface plasmon resonance (LSPR), which has been at the forefront of recent catalytic growth for oxidation, reduction, and coupling reaction.

The synthesized Ag NPs from *Botryococcus braunii* have 40–90 nm size revolved by SEM analysis and catalytic reduction of 2-nitroaniline to 2-(4-nitrophenyl)-1H-benzimidazole with a yield of 80% within 12 hours [197]. Moreover, *Aristolochia indica* was used to synthesize spherical Ag NPs implicated as a catalyst for the oxidation of benzyl alcohol to benzaldehyde; however, no oxidation reaction occurs at room temperature because secondary metabolites on the surface of nanoparticles retard the reaction. After heating the synthesized nanoparticles above 900°C, the stabilizing/capping agents are removed from the surface of nanoparticles and oxidation reaction occurs with a rate constant of $0.82 * 10^3\ M\ min^{-1}$ followed by zero-order kinetics [198]. Ag NPs synthesized using the stem extract of *Piper chaba* were found to be in almost spherical shape with a mean size of 19 nm by TEM analysis and reduction of 4-nitrophenol within 9 minutes [59]. Similarly, Ag NPs synthesized using *Zingiber officinale* display comparable catalytic activity on the reduction of 4-nitrophenol and can be reused effectively for at least five cycles with higher reduction efficiency [199]. Table 8 shows the morphology of green synthesized Ag NPs and their catalytic activity on different substrates.

7.9. Dye Degradation Activity. The presence of colored dyes in the discharged effluent reduces the penetration of light in the water bodies disturbing the photosynthesis and development of aqua communities [204]. Such dyes and their derivatives are particularly toxic, carcinogenic, and non-degradable, causing various complications such as skin infections and hepatic and kidney dysfunction and even damaging the living organism's nervous system [205]. Over the past few decades, various physical and chemical processes such as ultraviolet radiation [206], adsorption [207], electrochemical reduction [208], and advanced oxidation processes [209] have been developed to remove or degrade dyes in water. Most of these processes suffer from problems such as high prices and complex procedures, so it is critically necessary to create an environmentally sustainable and cost-effective solution for the deterioration of dyes in wastewater. The catalytic degradation of organic dyes using biologically synthesized nanoparticles can be employed [210]. The migration of electrons between Ag NPs and dye molecules plays a vital role in the degradation of dyes [211, 212].

The green synthesized nanoparticles using *Ekebergia capensis* showed good degradation activity against Allura red in less than 45 min and may involve electron relay mechanism [213]. The green synthesis of Ag NPs from *Terminalia arjuna* leaf exhibited strong degradation of the methyl orange (86.68%), methylene blue (93.60%), and Congo red (92.20%) by completing the reduction reaction within 20 minutes [11]. Ag NPs synthesized using *Vaccinium macrocarpon* fruit extract had spherical shape with size ranging from 15 to 30 nm as a catalyst for complete degradation of methyl orange, methylene blue, Rhodamine B, and Congo red within less than 300 seconds in the presence of sodium borohydride [214]. The biosynthesis of Ag NPs using *Polygonum hydropiper* extract and dye degradation effectiveness monitored for reduction of methylene blue in the presence of sodium borohydride showed a very fast reaction that changes the methylene blue into leucomethylene blue (colorless) within 13 minutes. However, sodium borohydride alone is unable to degrade the methylene blue as it is a strong reducing agent [215]. Table 9 shows the morphology of green synthesized Ag NPs and their dye degradation activity on different dyes.

7.10. Metal Sensing Activity. Heavy metals are naturally occurring materials present on the earth's surface, with much chemical degradation and human consumption arising from anthropogenic practices. Within plants and animals, the basic heavy metals perform oxidative and physiological roles [204, 219]. However, heavy metals have been reported to deteriorate the cellular organelles and components [220] within biological systems. Metal ion was observed to interfere with DNA, and nuclear proteins disrupt DNA and shifts in conformation [221]. There are several conventional methods to examine heavy metal concentration such as neutron activation analysis (NAA), atomic absorption spectroscopy (AAS), inductively coupled plasma mass spectroscopy (ICP-MS), and X-ray fluorescence spectrometry (XRF) [222], but such approaches must be supplemented with additional chromatographic techniques that are costly and time-consuming. Colorimetric metal sensing can be achieved *in situ* without any additional instruments using plasmonic Ag NPs. Ag NPs utilized in visual identification have characteristic SPR that is sensitive to the shape, size of the nanoparticle, and their local environment. This makes them a very suitable candidate for various optical sensing and detection applications such as heavy toxic metal sensing. The sensitivity of the nanoparticle towards the local environment depends on the morphology of the nanoparticles with rod shape (especially longer rods) and core shell (especially with thin metal shell) structure yielding a better SPR response monitored by using a UV-Vis spectrometer [223].

Apart from this, Ag NPs synthesized from various plant extracts have been used for optical sensing of various heavy metal ions. *Camellia sinensis* leaves were used to synthesize Ag NPs for the detection of Cu^{2+} and Pb^{2+} ions [224]. Ag

NPs were synthesized using leaves of *Amomum subulatum* for detection of Zn^{2+} in solution in the concentration range from $1 * 10^{-5}$ to $8 * 10^{-5}$ [225]. Ag NPs were synthesized using the aqueous extract from leaves of *Anacardium occidentale* for optical sensing of Cr^{6+} ions [226]. *Ginkgo biloba* leaf extract was used to synthesize Ag NPs as a fluorescence sensor for Cr^{4+} [139]. Table 10 shows the morphology of plant-mediated synthesis of Ag NPs, their metal sensing activity, and their detection limit.

7.11. The Hazardous Effect of Ag NPs in the Aquatic Biotic System. The use of Ag NPs in various potential applications is radically increasing day by day; however, numerous hazardous effects are only slowly recognized and evaluated in the aquatic biotic system [232, 233]. A huge amount of Ag NPs is synthesized every year by green and chemical as well as physical approaches. The green synthesized Ag NPs have lower toxicity than chemically synthesized nanoparticles. However, inappropriate disposal of nanoparticles in the environment resulting from either release during production and use or release after disposal of nanoparticle-containing products causes environmental fate due to aggregation, transformation, persistence, and sequestration leading to accumulation in the food chain and their consequences on human health [232, 234]. Different aquatic organisms directly face the toxicity of Ag NPs. Toxicity of Ag NPs in the aquatic system includes some test guidance such as acute immobilization test, acute toxicity test, and growth inhibition test estimated on median lethal concentrations/lethal concentration of Ag NPs [13]. Ag NPs induce toxicity, which largely depends on the particle surface properties, size, and exposure time which can be explained by the number of silver ions released from nanoparticles [235]. Table 11 shows the morphology of Ag NPs and their toxicity in different aquatic species.

8. Conclusion

Over the past decade, because of the diverse utility, Ag NPs have been more researched and synthesized. Green synthesis provides an ecofriendly one-pot strategy to synthesize biocompatible Ag NPs with a wide range of practical applications easily and cost effectively. The challenging parts of green synthetic strategy are method optimization to get the desirable size and stability of synthesized nanoparticles besides these identification of bioreducing secondary metabolites for silver salt that acts as either reducing agents or stabilizing and capping agents or both. Stronger secondary metabolites from the plant as reducing agents need to be identified, or new strategies need to be developed to increase the ability of existing green agents and to eliminate toxic reducing agents. Different factors affect the formation of nanoparticles, and a high concentration of silver salt causes deposition of salt on the Ag NPs and produces rough surfaces. Bioreduction of silver salt by different plants' secondary metabolites ranges from minutes up to 24 hours. The yield of nanoparticles and stability of Ag NPs increase with the increase in the incubation period. Secondary metabolites from plant sources play an important role in determining the morphology and stability of synthesized Ag NPs. Plant-mediated synthesis of Ag NPs has good biocompatibility and provides multifunctional applications in biological systems as well as catalysis and heavy metal sensing. In this study, we discussed the synthetic routes, characterization techniques, applications of plant-mediated Ag NPs, and their aquatic toxicity. Besides several advantages, there are some harmful effects of Ag NPs too, which are not covered extensively in this review.

Abbreviations

Ag NPs:	Silver nanoparticles
UV-Vis:	Ultraviolet visible
SPR:	Surface plasmon resonance
SERS:	Surface-enhanced Raman scattering
TEM:	Transmission electron microscopy
SEM:	Scanning electron microscopy
AFM:	Atomic force microscopy
DLS:	Dynamic light scattering
XRD:	X-ray diffraction
VSM:	Vibrating sample magnetometer
DNA:	Deoxyribonucleic acid
RNA:	Ribonucleic acid
ROS:	Reactive oxygen species
MIC:	Minimum inhibitory concentration
ZOI:	Zone of inhibition
MBC:	Minimum bactericidal concentration
SARS-CoV:	Severe acute respiratory syndrome coronavirus
HIV:	Human immunodeficiency virus
HBV:	Hepatitis B virus
IC_{50}:	Half maximal inhibitory concentration
MNTD:	Maximum nontoxic dose
$TCID_{50}$:	Median tissue culture infectious dose
DMSO:	Dimethyl sulfoxide
FCC:	Face-centered cubic
MIC_{50}:	Half minimum inhibitory concentration
MFC:	Minimum fungicidal concentration
BSA:	Bovine serum albumin
WHO:	World Health Organization
MTT:	3-[4,5-Dimethylthiazol-2-yl]-2,5 diphenyl tetrazolium bromide
LC:	Lethal concentration
LC_{50}:	Median lethal concentration
NAA:	Neutron activation analysis
AAS:	Atomic absorption spectroscopy
ICP-MS:	Inductively coupled plasma mass spectroscopy
XRF:	X-ray fluorescence spectrometry.

Data Availability

No data were used to support this study.

Conflicts of Interest

The authors declare that they have no conflicts of interest.

Authors' Contributions

All authors contributed equally to this study.

References

[1] F. Matteucci, R. Giannantonio, F. Calabi, A. Agostiano, G. Gigli, and M. Rossi, "Deployment and exploitation of nanotechnology nanomaterials and nanomedicine," *AIP Conference Proceedings*, vol. 1990, no. 1, Article ID 020001, 2018.

[2] M. Hekmati, S. Hasanirad, A. Khaledi, and D. Esmaeili, "Green synthesis of silver nanoparticles using extracts of *Allium rotundum, Falcaria vulgaris* Bernh, and *Ferulago angulate* Boiss, and their antimicrobial effects in vitro," *Gene Reports*, vol. 19, Article ID 100589, 2020.

[3] S. Ekrikaya, E. Yilmaz, C. Celik et al., "Investigation of ellagic acid rich-berry extracts directed silver nanoparticles synthesis and their antimicrobial properties with potential mechanisms towards *Enterococcus faecalis* and *Candida albicans*," *Journal of Biotechnology*, vol. 341, pp. 155–162, 2021.

[4] V. Sharma, S. Kaushik, P. Pandit, D. Dhull, J. P. Yadav, and S. Kaushik, "Green synthesis of silver nanoparticles from medicinal plants and evaluation of their antiviral potential against chikungunya virus," *Applied Microbiology and Biotechnology*, vol. 103, no. 2, pp. 881–891, 2019.

[5] S. Valsalam, P. Agastian, M. V. Arasu et al., "Rapid biosynthesis and characterization of silver nanoparticles from the leaf extract of *Tropaeolum majus* L. and its enhanced in-vitro antibacterial, antifungal, antioxidant and anticancer properties," *Journal of Photochemistry and Photobiology B: Biology*, vol. 191, pp. 65–74, 2019.

[6] P. Das, K. Ghosal, N. K. Jana, A. Mukherjee, and P. Basak, "Green synthesis and characterization of silver nanoparticles using belladonna mother tincture and its efficacy as a potential antibacterial and anti-inflammatory agent," *Materials Chemistry and Physics*, vol. 228, pp. 310–317, 2019.

[7] D. Jini and S. Sharmila, "Green synthesis of silver nanoparticles from *Allium cepa* and its *in vitro* antidiabetic activity," *Materials Today Proceedings*, vol. 22, pp. 432–438, 2020.

[8] O. Erdogan, M. Abbak, G. M. Demirbolat et al., "Green synthesis of silver nanoparticles via *Cynara scolymus* leaf extracts: the characterization, anticancer potential with photodynamic therapy in MCF7 cells," *PLoS One*, vol. 14, no. 6, Article ID e0216496, 2019.

[9] K. R. Aadil, N. Pandey, S. I. Mussatto, and H. Jha, "Green synthesis of silver nanoparticles using acacia lignin, their cytotoxicity, catalytic, metal ion sensing capability and antibacterial activity," *Journal of Environmental Chemical Engineering*, vol. 7, no. 5, Article ID 103296, 2019.

[10] Z. Wang, Y. Huang, D. Lv, G. Jiang, F. Zhang, and A. Song, "Tea polyphenol-assisted green synthesis of Ag-nano diamond hybrid and its catalytic activity towards 4-nitrophenol reduction," *Green Chemistry Letters and Reviews*, vol. 12, no. 3, pp. 197–207, 2019.

[11] S. Raj, H. Singh, R. Trivedi, and V. Soni, "Biogenic synthesis of AgNPs employing *Terminalia arjuna* leaf extract and its efficacy towards catalytic degradation of organic dyes," *Scientific Reports*, vol. 10, no. 1, Article ID 9616, 2020.

[12] M. N. Moore, "Do nanoparticles present ecotoxicological risks for the health of the aquatic environment?" *Environment International*, vol. 32, no. 8, pp. 967–976, 2006.

[13] E. K. Sohn, S. A. Johari, T. G. Kim et al., "Aquatic toxicity comparison of silver nanoparticles and silver nanowires," *BioMed Research International*, vol. 2015, Article ID 893049, 12 pages, 2015.

[14] S. Lekamge, A. F. Miranda, A. Abraham et al., "The toxicity of silver nanoparticles (AgNPs) to three freshwater invertebrates with different life strategies: *Hydra vulgaris, Daphnia carinata*, and *Paratya australiensis*," *Frontiers in Environmental Science*, vol. 6, p. 152, 2018.

[15] X. Duan, D. Peng, Y. Zhang et al., "Sub-cytotoxic concentrations of ionic silver promote the proliferation of human keratinocytes by inducing the production of reactive oxygen species," *Frontiers of Medicine*, vol. 12, no. 3, pp. 289–300, 2018.

[16] S. Kittler, C. Greulich, J. Diendorf, M. Köller, and M. Epple, "Toxicity of silver nanoparticles increases during storage because of slow dissolution under release of silver ions," *Chemistry of Materials*, vol. 22, no. 16, pp. 4548–4554, 2010.

[17] H. J. Yen, S. h. Hsu, and C. L. Tsai, "Cytotoxicity and immunological response of gold and silver nanoparticles of different sizes," *Small*, vol. 5, no. 13, pp. 1553–1561, 2009.

[18] H.-J. Eom and J. Choi, "p38 MAPK activation, DNA damage, cell cycle arrest and apoptosis as mechanisms of toxicity of silver nanoparticles in Jurkat T cells," *Environmental Science & Technology*, vol. 44, no. 21, pp. 8337–8342, 2010.

[19] Y. Choi, H.-A. Kim, K.-W. Kim, and B.-T. Lee, "Comparative toxicity of silver nanoparticles and silver ions to *Escherichia coli*," *Journal of Environmental Sciences*, vol. 66, pp. 50–60, 2018.

[20] I. Khan, A. Bahuguna, M. Krishnan et al., "The effect of biogenic manufactured silver nanoparticles on human endothelial cells and zebrafish model," *The Science of the Total Environment*, vol. 679, pp. 365–377, 2019.

[21] L. Xu, Y.-Y. Wang, J. Huang, C.-Y. Chen, Z.-X. Wang, and H. Xie, "Silver nanoparticles: synthesis, medical applications and biosafety," *Theranostics*, vol. 10, no. 20, pp. 8996–9031, 2020.

[22] M. Akter, M. T. Sikder, M. M. Rahman et al., "A systematic review on silver nanoparticles-induced cytotoxicity: physicochemical properties and perspectives," *Journal of Advanced Research*, vol. 9, pp. 1–16, 2018.

[23] N. L. Pacioni, C. D. Borsarelli, V. Rey, and A. V. Veglia, "Synthetic routes for the preparation of silver nanoparticles," in *Silver Nanoparticle Applications*, E. I. Alarcon, M. Griffith, and K. I. Udekwu, Eds., Springer International Publishing, Cham, Switzerland, pp. 13–46, 2015.

[24] M. H. Magnusson, K. Deppert, J.-O. Malm, J.-O. Bovin, and L. Samuelson, "Gold nanoparticles: production, reshaping, and thermal charging," *Journal of Nanoparticle Research*, vol. 1, no. 2, pp. 243–251, 1999.

[25] F. E. Kruis, H. Fissan, and B. Rellinghaus, "Sintering and evaporation characteristics of gas-phase synthesis of size-selected PbS nanoparticles," *Materials Science and Engineering: B*, vol. 69-70, pp. 329–334, 2000.

[26] M. Raffi, A. K. Rumaiz, M. M. Hasan, and S. I. Shah, "Studies of the growth parameters for silver nanoparticle synthesis by inert gas condensation," *Journal of Materials Research*, vol. 22, no. 12, pp. 3378–3384, 2007.

[27] A. Pyatenko, K. Shimokawa, M. Yamaguchi, O. Nishimura, and M. Suzuki, "Synthesis of silver nanoparticles by laser ablation in pure water," *Applied Physics A*, vol. 79, no. 4-6, pp. 803–806, 2004.

[28] Y.-H. Chen and C.-S. Yeh, "Laser ablation method: use of surfactants to form the dispersed Ag nanoparticles," *Colloids*

and Surfaces A: Physicochemical and Engineering Aspects, vol. 197, no. 1–3, pp. 133–139, 2002.

[29] J. Lu, J. Guo, S. Song et al., "Preparation of Ag nanoparticles by spark ablation in gas as catalysts for electrocatalytic hydrogen production," *RSC Advances*, vol. 10, no. 63, pp. 38583–38587, 2020.

[30] R. Güzel and G. Erdal, "Synthesis of silver nanoparticles," in *Silver Nanoparticles-Fabrication, Characterization and Applications*, K. Maaz, Ed., InTech, London, UK, 2018.

[31] M. Raza, Z. Kanwal, A. Rauf, A. Sabri, S. Riaz, and S. Naseem, "Size- and shape-dependent antibacterial studies of silver nanoparticles synthesized by wet chemical routes," *Nanomaterials*, vol. 6, no. 4, p. 74, 2016.

[32] V. Demchenko, S. Riabov, S. Kobylinskyi et al., "Effect of the type of reducing agents of silver ions in interpolyelectrolyte-metal complexes on the structure, morphology and properties of silver-containing nanocomposites," *Scientific Reports*, vol. 10, no. 1, Article ID 7126, 2020.

[33] S. Anil Kumar, M. K. Abyaneh, S. W. Gosavi et al., "Nitrate reductase-mediated synthesis of silver nanoparticles from AgNO3," *Biotechnology Letters*, vol. 29, no. 3, pp. 439–445, 2007.

[34] T. Chen, I. Öçsoy, Q. Yuan et al., "One-Step facile surface engineering of hydrophobic nanocrystals with designer molecular recognition," *Journal of the American Chemical Society*, vol. 134, no. 32, pp. 13164–13167, 2012.

[35] I. Ocsoy, B. Gulbakan, T. Chen et al., "DNA-guided metal-nanoparticle formation on graphene oxide surface," *Advanced Materials*, vol. 25, no. 16, pp. 2319–2325, 2013.

[36] I. Ocsoy, D. Tasdemir, S. Mazicioglu, C. Celik, A. Katı, and F. Ulgen, "Biomolecules incorporated metallic nanoparticles synthesis and their biomedical applications," *Materials Letters*, vol. 212, pp. 45–50, 2018.

[37] I. Ocsoy, M. L. Paret, M. A. Ocsoy et al., "Nanotechnology in plant disease management: DNA-directed silver nanoparticles on graphene oxide as an antibacterial against *Xanthomonas perforans*," *ACS Nano*, vol. 7, no. 10, pp. 8972–8980, 2013.

[38] A. Strayer, I. Ocsoy, W. Tan, J. B. Jones, and M. L. Paret, "Low concentrations of a silver-based nanocomposite to manage bacterial spot of tomato in the greenhouse," *Plant Disease*, vol. 100, no. 7, pp. 1460–1465, 2016.

[39] D. Turek, D. Van Simaeys, J. Johnson, I. Ocsoy, and W. Tan, "Molecular recognition of live methicillin-resistant *Staphylococcus aureus* cells using DNA aptamers," *World Journal of Translational Medicine*, vol. 2, no. 3, pp. 67–74, 2013.

[40] Y. Leng, L. Fu, L. Ye et al., "Protein-directed synthesis of highly monodispersed, spherical gold nanoparticles and their applications in multidimensional sensing," *Scientific Reports*, vol. 6, no. 1, Article ID 28900, 2016.

[41] H. Fouad, L. Hongjie, D. Yanmei et al., "Synthesis and characterization of silver nanoparticles using *Bacillus amyloliquefaciens* and *Bacillus subtilis* to control filarial vector *Culex pipiens pallens* and its antimicrobial activity," *Artificial Cells, Nanomedicine, and Biotechnology*, vol. 45, no. 7, pp. 1369–1378, 2017.

[42] C. G. Kumar and S. K. Mamidyala, "Extracellular synthesis of silver nanoparticles using culture supernatant of *Pseudomonas aeruginosa*," *Colloids and Surfaces B: Biointerfaces*, vol. 84, no. 2, pp. 462–466, 2011.

[43] K. Divya, L. C. Kurian, S. Vijayan, and J. Manakulam Shaikmoideen, "Green synthesis of silver nanoparticles by *Escherichia coli*: analysis of antibacterial activity," *Journal of Water and Environmental Nanotechnology*, vol. 1, no. 1, pp. 63–74, 2016.

[44] B. A. Chopade, R. Singh, P. Wagh et al., "Synthesis, optimization, and characterization of silver nanoparticles from *Acinetobacter calcoaceticus* and their enhanced antibacterial activity when combined with antibiotics," *International Journal of Nanomedicine*, vol. 8, pp. 4277–4290, 2013.

[45] D. Cruz, P. L. Falé, A. Mourato, P. D. Vaz, M. Luisa Serralheiro, and A. R. L. Lino, "Preparation and physicochemical characterization of Ag nanoparticles biosynthesized by *Lippia citriodora* (Lemon Verbena)," *Colloids and Surfaces B: Biointerfaces*, vol. 81, no. 1, pp. 67–73, 2010.

[46] S. Chouhan and S. Guleria, "Green synthesis of AgNPs using *Cannabis sativa* leaf extract: characterization, antibacterial, anti-yeast and α-amylase inhibitory activity," *Materials Science for Energy Technologies*, vol. 3, pp. 536–544, 2020.

[47] J. Baharara, F. Namvar, M. Mousavi, T. Ramezani, and R. Mohamad, "Anti-angiogenesis effect of biogenic silver nanoparticles synthesized using *Saliva officinalis* on chick chorioalantoic membrane (CAM)," *Molecules*, vol. 19, no. 9, pp. 13498–13508, 2014.

[48] H. Bar, D. K. Bhui, G. P. Sahoo, P. Sarkar, S. Pyne, and A. Misra, "Green synthesis of silver nanoparticles using seed extract of *Jatropha curcas*," *Colloids and Surfaces A: Physicochemical and Engineering Aspects*, vol. 348, no. 1-3, pp. 212–216, 2009.

[49] K. Jeeva, M. Thiyagarajan, V. Elangovan, N. Geetha, and P. Venkatachalam, "*Caesalpinia coriaria* leaf extracts mediated biosynthesis of metallic silver nanoparticles and their antibacterial activity against clinically isolated pathogens," *Industrial Crops and Products*, vol. 52, pp. 714–720, 2014.

[50] M. Vijayakumar, K. Priya, F. T. Nancy, A. Noorlidah, and A. B. A. Ahmed, "Biosynthesis, characterisation and antibacterial effect of plant-mediated silver nanoparticles using *Artemisia nilagirica*," *Industrial Crops and Products*, vol. 41, pp. 235–240, 2013.

[51] I. Fatimah, "Green synthesis of silver nanoparticles using extract of *Parkia speciosa* Hassk pods assisted by microwave irradiation," *Journal of Advanced Research*, vol. 7, no. 6, pp. 961–969, 2016.

[52] M. Sathishkumar, K. Sneha, S. W. Won, C.-W. Cho, S. Kim, and Y.-S. Yun, "*Cinnamon zeylanicum* Bark extract and powder mediated green synthesis of nano-crystalline silver particles and its bactericidal activity," *Colloids and Surfaces B: Biointerfaces*, vol. 73, no. 2, pp. 332–338, 2009.

[53] D. Garibo, H. A. Borbón-Nuñez, J. N. D. de León et al., "Green synthesis of silver nanoparticles using *Lysiloma acapulcensis* exhibit high-antimicrobial activity," *Scientific Reports*, vol. 10, no. 1, Article ID 12805, 2020.

[54] A. A. Zahir, I. S. Chauhan, A. Bagavan et al., "Green synthesis of silver and titanium dioxide nanoparticles using *Euphorbia prostrata* extract shows shift from apoptosis to G_0/G_1 arrest followed by necrotic cell death in *Leishmania donovani*," *Antimicrobial Agents and Chemotherapy*, vol. 59, no. 8, pp. 4782–4799, 2015.

[55] S. M. Roopan, Rohit, G. Madhumitha et al., "Low-cost and eco-friendly phyto-synthesis of silver nanoparticles using *Cocos nucifera* coir extract and its larvicidal activity," *Industrial Crops and Products*, vol. 43, pp. 631–635, 2013.

[56] W. R. Rolim, M. T. Pelegrino, B. de Araújo Lima et al., "Green tea extract mediated biogenic synthesis of silver nanoparticles: characterization, cytotoxicity evaluation and

antibacterial activity," *Applied Surface Science*, vol. 463, pp. 66–74, 2019.

[57] R. Ceylan, A. Demirbas, I. Ocsoy, and A. Aktumsek, "Green synthesis of silver nanoparticles using aqueous extracts of three Sideritis species from Turkey and evaluations bioactivity potentials," *Sustainable Chemistry and Pharmacy*, vol. 21, Article ID 100426, 2021.

[58] S. Pugazhendhi, "Synthesis of *Ipomoea staphylina* plant extract mediated silver nanoparticles," *Materials Today Proceedings*, vol. 33, pp. 4626–4629, 2020.

[59] M. Mahiuddin, P. Saha, and B. Ochiai, "Green synthesis and catalytic activity of silver nanoparticles based on *Piper chaba* stem extracts," *Nanomaterials*, vol. 10, no. 9, Article ID 1777, 2020.

[60] G. Marslin, K. Siram, Q. Maqbool et al., "Secondary metabolites in the green synthesis of metallic nanoparticles," *Materials*, vol. 11, no. 6, p. 940, 2018.

[61] N. Ahmad, S. Sharma, M. K. Alam et al., "Rapid synthesis of silver nanoparticles using dried medicinal plant of Basil," *Colloids and Surfaces B: Biointerfaces*, vol. 81, no. 1, pp. 81–86, 2010.

[62] S. Ahmed, M. Ahmad, B. L. Swami, and S. Ikram, "A review on plants extract mediated synthesis of silver nanoparticles for antimicrobial applications: a green expertise," *Journal of Advanced Research*, vol. 7, no. 1, pp. 17–28, 2016.

[63] S. Some, O. Bulut, K. Biswas et al., "Effect of feed supplementation with biosynthesized silver nanoparticles using leaf extract of *Morus indica* L. V1 on *Bombyx mori* L. (*Lepidoptera: Bombycidae*)," *Scientific Reports*, vol. 9, no. 1, Article ID 14839, 2019.

[64] S. Iravani, "Green synthesis of metal nanoparticles using plants," *Green Chemistry*, vol. 13, no. 10, Article ID 2638, 2011.

[65] O. V. Mikhailov and E. O. Mikhailova, "Elemental silver nanoparticles: biosynthesis and bio applications," *Materials*, vol. 12, no. 19, Article ID 3177, 2019.

[66] H. M. M. Ibrahim, "Green synthesis and characterization of silver nanoparticles using banana peel extract and their antimicrobial activity against representative microorganisms," *Journal of Radiation Research and Applied Sciences*, vol. 8, no. 3, pp. 265–275, 2015.

[67] R. Prasad, "Synthesis of silver nanoparticles in photosynthetic plants," *Journal of Nanoparticles*, vol. 2014, Article ID 963961, 8 pages, 2014.

[68] M. K. Alqadi, O. A. Abo Noqtah, F. Y. Alzoubi, J. Alzouby, and K. Aljarrah, "pH effect on the aggregation of silver nanoparticles synthesized by chemical reduction," *Materials Science-Poland*, vol. 32, no. 1, pp. 107–111, 2014.

[69] P. Li, S. Li, Y. Wang, Y. Zhang, and G.-Z. Han, "Green synthesis of β-CD-functionalized monodispersed silver nanoparticles with ehanced catalytic activity," *Colloids and Surfaces A: Physicochemical and Engineering Aspects*, vol. 520, pp. 26–31, 2017.

[70] C. K. Tagad, S. R. Dugasani, R. Aiyer, S. Park, A. Kulkarni, and S. Sabharwal, "Green synthesis of silver nanoparticles and their application for the development of optical fiber based hydrogen peroxide sensor," *Sensors and Actuators B: Chemical*, vol. 183, pp. 144–149, 2013.

[71] J. A. Wisam and A. J. Haneen, "A novel study of pH influence on Ag nanoparticles size with antibacterial and antifungal activity using green synthesis," *World Scientific News*, vol. 97, pp. 139–152, 2018.

[72] H. Liu, H. Zhang, J. Wang, and J. Wei, "Effect of temperature on the size of biosynthesized silver nanoparticle: deep insight into microscopic kinetics analysis," *Arabian Journal of Chemistry*, vol. 13, no. 1, pp. 1011–1019, 2020.

[73] M. Ndikau, N. M. Noah, D. M. Andala, and E. Masika, "Green synthesis and characterization of silver nanoparticles using *Citrullus lanatus* fruit rind extract," *International Journal of Analytical Chemistry*, vol. 2017, Article ID 8108504, 9 pages, 2017.

[74] A. O. Dada, A. A. Inyinbor, E. I. Idu et al., "Effect of operational parameters, characterization and antibacterial studies of green synthesis of silver nanoparticles using *Tithonia diversifolia*," *PeerJ*, vol. 6, Article ID e5865, 2018.

[75] M. Darroudi, "Time-dependent effect in green synthesis of silver nanoparticles," *International Journal of Nanomedicine*, vol. 6, pp. 677–681, 2011.

[76] I. Ocsoy, A. Demirbas, E. S. McLamore, B. Altinsoy, N. Ildiz, and A. Baldemir, "Green synthesis with incorporated hydrothermal approaches for silver nanoparticles formation and enhanced antimicrobial activity against bacterial and fungal pathogens," *Journal of Molecular Liquids*, vol. 238, pp. 263–269, 2017.

[77] A. Gupta, A. R. Koirala, B. Gupta, and N. Parajuli, "Improved method for separation of silver nanoparticles synthesized using the *Nyctanthes arbor-tristis* shrub," *Acta Chemica Malaysia*, vol. 3, no. 1, pp. 35–42, 2019.

[78] R. A. Hamouda, M. H. Hussein, R. A. Abo-Elmagd, and S. S. Bawazir, "Synthesis and biological characterization of silver nanoparticles derived from the cyanobacterium *Oscillatoria limnetica*," *Scientific Reports*, vol. 9, no. 1, Article ID 13071, 2019.

[79] P. R. M. Hemlata, P. R. Meena, A. P. Singh, and K. K. Tejavath, "Biosynthesis of silver nanoparticles using *Cucumis prophetarum* aqueous leaf extract and their antibacterial and antiproliferative activity against cancer cell lines," *ACS Omega*, vol. 5, no. 10, pp. 5520–5528, 2020.

[80] J. M. Ashraf, M. A. Ansari, H. M. Khan, M. A. Alzohairy, and I. Choi, "Green synthesis of silver nanoparticles and characterization of their inhibitory effects on AGEs formation using biophysical techniques," *Scientific Reports*, vol. 6, no. 1, Article ID 20414, 2016.

[81] Y.-G. Zhou, N. V. Rees, and R. G. Compton, "The electrochemical detection and characterization of silver nanoparticles in aqueous solution," *Angewandte Chemie International Edition*, vol. 50, no. 18, pp. 4219–4221, 2011.

[82] Y. Li, S.-M. Chen, M. A. Ali, and F. M. A. AlHemaid, "Biosynthesis and electrochemical characterization of silver nanoparticles from leaf extract of *Adenium obesum* and its application to antibacterial effect," *International Journal of Electrochemical Science*, vol. 8, pp. 2691–2701, 2013.

[83] S. L. Pal, U. Jana, P. K. Manna, G. P. Mohanta, and R. Manavalan, "Nanoparticle: an overview of preparation and characterization," *Journal of Applied Pharmaceutical Science*, vol. 1, no. 6, pp. 228–234, 2011.

[84] Y. Yang, W. Song, Z. Chen, Q. Li, and L. Liu, "Ameliorative effect of synthesized silver nanoparticles by green route method from *Zingiber zerumbet* on *mycoplasmal pneumonia* in experimental mice," *Artificial Cells, Nanomedicine, and Biotechnology*, vol. 47, no. 1, pp. 2146–2154, 2019.

[85] K. K. Bharadwaj, B. Rabha, S. Pati et al., "Green synthesis of silver nanoparticles using *Diospyros malabarica* fruit extract and assessments of their antimicrobial, anticancer and catalytic reduction of 4-nitrophenol (4-NP)," *Nanomaterials*, vol. 11, no. 8, Article ID 1999, 2021.

[86] S. Mahmood, U. K. Mandal, B. Chatterjee, and M. Taher, "Advanced characterizations of nanoparticles for drug

delivery: investigating their properties through the techniques used in their evaluations," *Nanotechnology Reviews*, vol. 6, no. 4, pp. 355–372, 2017.

[87] P. Banerjee, M. Satapathy, A. Mukhopahayay, and P. Das, "Leaf extract mediated green synthesis of silver nanoparticles from widely available Indian plants: synthesis, characterization, antimicrobial property and toxicity analysis," *Bioresources and Bioprocessing*, vol. 1, no. 1, p. 3, 2014.

[88] M. Bhagat, R. Anand, R. Datt, V. Gupta, and S. Arya, "Green synthesis of silver nanoparticles using aqueous extract of *Rosa brunonii* Lindl and their morphological, biological and photocatalytic characterizations," *Journal of Inorganic and Organometallic Polymers and Materials*, vol. 29, no. 3, pp. 1039–1047, 2019.

[89] A. Alahmad, A. Feldhoff, N. C. Bigall, P. Rusch, T. Scheper, and J.-G. Walter, "*Hypericum perforatum* L.-mediated green synthesis of silver nanoparticles exhibiting antioxidant and anticancer activities," *Nanomaterials*, vol. 11, no. 2, Article ID 487, 2021.

[90] C. Kumar, P. Yugandhar, and N. Savithramma, "Biological synthesis of silver nanoparticles from *Adansonia digitata* L. fruit pulp extract, characterization, and its antimicrobial properties," *Journal of Intercultural Ethnopharmacology*, vol. 5, no. 1, pp. 79–85, 2016.

[91] Y. Mao, K. Liu, C. Zhan, L. Geng, B. Chu, and B. S. Hsiao, "Characterization of nanocellulose using small-angle neutron, x-ray, and dynamic light scattering techniques," *The Journal of Physical Chemistry B*, vol. 121, no. 6, pp. 1340–1351, 2017.

[92] J. Stetefeld, S. A. McKenna, and T. R. Patel, "Dynamic light scattering: a practical guide and applications in biomedical sciences," *Biophysical Reviews*, vol. 8, no. 4, pp. 409–427, 2016.

[93] H. Erjaee, H. Rajaian, and S. Nazifi, "Synthesis and characterization of novel silver nanoparticles using *Chamaemelum nobile* extract for antibacterial application," *Advances in Natural Sciences: Nanoscience and Nanotechnology*, vol. 8, no. 2, Article ID 025004, 2017.

[94] J. K. Patra, G. Das, and H.-S. Shin, "Facile green biosynthesis of silver nanoparticles using *Pisum sativum* L. outer peel aqueous extract and its antidiabetic, cytotoxicity, antioxidant, and antibacterial activity," *International Journal of Nanomedicine*, vol. 14, pp. 6679–6690, 2019.

[95] S. Samimi, N. Maghsoudnia, R. B. Eftekhari, and F. Dorkoosh, "Lipid-based nanoparticles for drug delivery systems," in *Characterization and Biology of Nanomaterials for Drug Delivery*, pp. 47–76, Elsevier, Amsterdam, Netherlands, 2019.

[96] R. Verkhovskii, A. Kozlova, V. Atkin, R. Kamyshinsky, T. Shulgina, and O. Nechaeva, "Physical properties and cytotoxicity of silver nanoparticles under different polymeric stabilizers," *Heliyon*, vol. 5, no. 3, Article ID e01305, 2019.

[97] R. Vivek, R. Thangam, K. Muthuchelian, P. Gunasekaran, K. Kaveri, and S. Kannan, "Green biosynthesis of silver nanoparticles from *Annona squamosa* leaf extract and its *in vitro* cytotoxic effect on MCF-7 cells," *Process Biochemistry*, vol. 47, no. 12, pp. 2405–2410, 2012.

[98] B. K. Mehta, M. Chhajlani, and B. D. Shrivastava, "Green synthesis of silver nanoparticles and their characterization by XRD," *Journal of Physics: Conference Series*, vol. 836, Article ID 012050, 2017.

[99] L. M. Moreau, D.-H. Ha, H. Zhang, R. Hovden, D. A. Muller, and R. D. Robinson, "Defining crystalline/amorphous phases of nanoparticles through X-ray absorption spectroscopy and X-ray diffraction: the case of nickel phosphide," *Chemistry of Materials*, vol. 25, no. 12, pp. 2394–2403, 2013.

[100] M. S. Akhtar, J. Panwar, and Y.-S. Yun, "Biogenic synthesis of metallic nanoparticles by plant extracts," *ACS Sustainable Chemistry & Engineering*, vol. 1, no. 6, pp. 591–602, 2013.

[101] B. Bhattarai, Y. Zaker, and T. P. Bigioni, "Green synthesis of gold and silver nanoparticles: challenges and opportunities," *Current Opinion in Green and Sustainable Chemistry*, vol. 12, pp. 91–100, 2018.

[102] A. Desireddy, B. E. Conn, J. Guo et al., "Ultrastable silver nanoparticles," *Nature*, vol. 501, no. 7467, pp. 399–402, 2013.

[103] Y. Negishi, K. Nobusada, and T. Tsukuda, "Glutathione-protected gold clusters revisited: bridging the gap between gold(I)-thiolate complexes and thiolate-protected gold nanocrystals," *Journal of the American Chemical Society*, vol. 127, no. 14, pp. 5261–5270, 2005.

[104] J. S. Kim, E. Kuk, K. N. Yu et al., "Antimicrobial effects of silver nanoparticles," *Nanomedicine: Nanotechnology, Biology and Medicine*, vol. 3, no. 1, pp. 95–101, 2007.

[105] G. Madhumitha, G. Elango, and S. M. Roopan, "Bio-functionalized doped silver nanoparticles and its antimicrobial studies," *Journal of Sol-Gel Science and Technology*, vol. 73, no. 2, pp. 476–483, 2015.

[106] M. Bilal, T. Rasheed, H. M. N. Iqbal, H. Hu, and X. Zhang, "Silver nanoparticles: biosynthesis and antimicrobial potentialities," *International Journal of Pharmacology*, vol. 13, no. 7, pp. 832–845, 2017.

[107] T. C. Dakal, A. Kumar, R. S. Majumdar, and V. Yadav, "Mechanistic basis of antimicrobial actions of silver nanoparticles," *Frontiers in Microbiology*, vol. 7, 2016.

[108] A. K. Keshari, R. Srivastava, P. Singh, V. B. Yadav, and G. Nath, "Antioxidant and antibacterial activity of silver nanoparticles synthesized by *Cestrum nocturnum*," *Journal of Ayurveda and Integrative Medicine*, vol. 11, no. 1, pp. 37–44, 2020.

[109] T. Dutta, N. N. Ghosh, M. Das, R. Adhikary, V. Mandal, and A. P. Chattopadhyay, "Green synthesis of antibacterial and antifungal silver nanoparticles using *Citrus limetta* peel extract: experimental and theoretical studies," *Journal of Environmental Chemical Engineering*, vol. 8, no. 4, Article ID 104019, 2020.

[110] M. R. Bindhu, M. Umadevi, G. A. Esmail, N. A. Al-Dhabi, and M. V. Arasu, "Green synthesis and characterization of silver nanoparticles from *Moringa oleifera* flower and assessment of antimicrobial and sensing properties," *Journal of Photochemistry and Photobiology B: Biology*, vol. 205, Article ID 111836, 2020.

[111] A. Nouri, M. Tavakkoli Yaraki, A. Lajevardi, Z. Rezaei, M. Ghorbanpour, and M. Tanzifi, "Ultrasonic-assisted green synthesis of silver nanoparticles using *Mentha aquatica* leaf extract for enhanced antibacterial properties and catalytic activity," *Colloid and Interface Science Communications*, vol. 35, Article ID 100252, 2020.

[112] M. N. Lakhan, R. Chen, A. H. Shar et al., "Eco-friendly green synthesis of clove buds extract functionalized silver nanoparticles and evaluation of antibacterial and antidiatom activity," *Journal of Microbiological Methods*, vol. 173, Article ID 105934, 2020.

[113] M. Maghimaa and S. A. Alharbi, "Green synthesis of silver nanoparticles from *Curcuma longa* L. and coating on the cotton fabrics for antimicrobial applications and wound healing activity," *Journal of Photochemistry and Photobiology B: Biology*, vol. 204, Article ID 111806, 2020.

[114] M. L. Guimarães, F. A. G. da Silva, M. M. da Costa, and H. P. de Oliveira, "Green synthesis of silver nanoparticles using *Ziziphus joazeiro* leaf extract for production of antibacterial agents," *Applied Nanoscience*, vol. 10, no. 4, pp. 1073–1081, 2020.

[115] M. Devi, S. Devi, V. Sharma, N. Rana, R. K. Bhatia, and A. K. Bhatt, "Green synthesis of silver nanoparticles using methanolic fruit extract of *Aegle marmelos* and their antimicrobial potential against human bacterial pathogens," *Journal of Traditional and Complementary Medicine*, vol. 10, no. 2, pp. 158–165, 2020.

[116] R. Mariselvam, A. J. A. Ranjitsingh, A. Usha Raja Nanthini, K. Kalirajan, C. Padmalatha, and P. Mosae Selvakumar, "Green synthesis of silver nanoparticles from the extract of the inflorescence of *Cocos nucifera* (Family: Arecaceae) for enhanced antibacterial activity," *Spectrochimica Acta Part A: Molecular and Biomolecular Spectroscopy*, vol. 129, pp. 537–541, 2014.

[117] F. Esmaile, H. Koohestani, and H. Abdollah-Pour, "Characterization and antibacterial activity of silver nanoparticles green synthesized using *Ziziphora clinopodioides* extract," *Environmental Nanotechnology, Monitoring & Management*, vol. 14, Article ID 100303, 2020.

[118] A. Rautela, J. Rani, and M. Debnath, "Green synthesis of silver nanoparticles from *Tectona grandis* seeds extract: characterization and mechanism of antimicrobial action on different microorganisms," *Journal of Analytical Science and Technology*, vol. 10, no. 1, p. 5, 2019.

[119] M. Hamelian, M. M. Zangeneh, A. Amisama, K. Varmira, and H. Veisi, "Green synthesis of silver nanoparticles using *Thymus kotschyanus* extract and evaluation of their antioxidant, antibacterial and cytotoxic effects," *Applied Organometallic Chemistry*, vol. 32, no. 9, Article ID e4458, 2018.

[120] P. P. N. Vijay Kumar, S. V. N. Pammi, P. Kollu, K. V. V. Satyanarayana, and U. Shameem, "Green synthesis and characterization of silver nanoparticles using *Boerhaavia diffusa* plant extract and their anti bacterial activity," *Industrial Crops and Products*, vol. 52, pp. 562–566, 2014.

[121] R. J. Coker, B. M. Hunter, J. W. Rudge, M. Liverani, and P. Hanvoravongchai, "Emerging infectious diseases in southeast Asia: regional challenges to control," *The Lancet*, vol. 377, no. 9765, pp. 599–609, 2011.

[122] A. Salleh, R. Naomi, N. D. Utami et al., "The potential of silver nanoparticles for antiviral and antibacterial applications: a mechanism of action," *Nanomaterials*, vol. 10, no. 8, Article ID 1566, 2020.

[123] M. Rai, S. D. Deshmukh, A. P. Ingle, I. R. Gupta, M. Galdiero, and S. Galdiero, "Metal nanoparticles: the protective nanoshield against virus infection," *Critical Reviews in Microbiology*, vol. 42, no. 1, pp. 46–56, 2016.

[124] J. L. Elechiguerra, J. L. Burt, J. R. Morones et al., "Interaction of silver nanoparticles with HIV-1," *Journal of Nanobiotechnology*, vol. 3, no. 1, p. 6, 2005.

[125] T. V. M. Sreekanth, P. C. Nagajyothi, P. Muthuraman et al., "Ultra-sonication-assisted silver nanoparticles using *Panax ginseng* root extract and their anti-cancer and antiviral activities," *Journal of Photochemistry and Photobiology B: Biology*, vol. 188, pp. 6–11, 2018.

[126] S. D. Kumar, G. Singaravelu, S. Ajithkumar, K. Murugan, M. Nicoletti, and G. Benelli, "Mangrove-mediated green synthesis of silver nanoparticles with high HIV-1 reverse transcriptase inhibitory potential," *Journal of Cluster Science*, vol. 28, no. 1, pp. 359–367, 2017.

[127] E. Haggag, A. Elshamy, M. Rabeh et al., "Antiviral potential of green synthesized silver nanoparticles of *Lampranthus coccineus* and *Malephora lutea*," *International Journal of Nanomedicine*, vol. 14, pp. 6217–6229, 2019.

[128] V. Sujitha, K. Murugan, M. Paulpandi et al., "Green-synthesized silver nanoparticles as a novel control tool against dengue virus (DEN-2) and its primary vector *Aedes aegypti*," *Parasitology Research*, vol. 114, no. 9, pp. 3315–3325, 2015.

[129] S. Choudhary, R. Kumar, U. Dalal, S. Tomar, and S. N. Reddy, "Green synthesis of nanometal impregnated biomass-antiviral potential," *Materials Science and Engineering: C*, vol. 112, Article ID 110934, 2020.

[130] M. Fatima, N.-u.-S. S. Zaidi, and D. Amraiz, "*In vitro* antiviral activity of *Cinnamomum cassia* and its nanoparticles against H7N3 influenza A virus," *Journal of Microbiology and Biotechnology*, vol. 26, no. 1, pp. 151–159, 2016.

[131] D. A. Enoch, H. A. Ludlam, and N. M. Brown, "Invasive fungal infections: a review of epidemiology and management options," *Journal of Medical Microbiology*, vol. 55, no. 7, pp. 809–818, 2006.

[132] S. V. Otari, R. M. Patil, S. J. Ghosh, N. D. Thorat, and S. H. Pawar, "Intracellular synthesis of silver nanoparticle by actinobacteria and its antimicrobial activity," *Spectrochimica Acta Part A: Molecular and Biomolecular Spectroscopy*, vol. 136, pp. 1175–1180, 2015.

[133] Z.-K. Xia, Q.-H. Ma, S.-Y. Li et al., "The antifungal effect of silver nanoparticles on *Trichosporon asahii*," *Journal of Microbiology, Immunology, and Infection*, vol. 49, no. 2, pp. 182–188, 2016.

[134] K.-J. Lee, S.-H. Park, M. Govarthanan et al., "Synthesis of silver nanoparticles using cow milk and their antifungal activity against phytopathogens," *Materials Letters*, vol. 105, pp. 128–131, 2013.

[135] E. J. J. Mallmann, F. A. Cunha, B. N. M. F. Castro, A. M. Maciel, E. A. Menezes, and P. B. A. Fechine, "Antifungal activity of silver nanoparticles obtained by green synthesis," *Revista do Instituto de Medicina Tropical de São Paulo*, vol. 57, no. 2, pp. 165–167, 2015.

[136] S. Mahadevan, S. Vijayakumar, and P. Arulmozhi, "Green synthesis of silver nano particles from *Atalantia monophylla* (L) Correa leaf extract, their antimicrobial activity and sensing capability of H_2O_2," *Microbial Pathogenesis*, vol. 113, pp. 445–450, 2017.

[137] S. Ghojavand, M. Madani, and J. Karimi, "Green synthesis, characterization and antifungal activity of silver nanoparticles using stems and flowers of felty germander," *Journal of Inorganic and Organometallic Polymers and Materials*, vol. 30, no. 8, pp. 2987–2997, 2020.

[138] G. N. Maity, P. Maity, I. Choudhuri et al., "Green synthesis, characterization, antimicrobial and cytotoxic effect of silver nanoparticles using arabinoxylan isolated from Kalmegh," *International Journal of Biological Macromolecules*, vol. 162, pp. 1025–1034, 2020.

[139] W. Huang, M. Yan, H. Duan, Y. Bi, X. Cheng, and H. Yu, "Synergistic antifungal activity of green synthesized silver nanoparticles and epoxiconazole against *Setosphaeria turcica*," *Journal of Nanomaterials*, vol. 2020, Article ID 9535432, 7 pages, 2020.

[140] B. Bahrami-Teimoori, Y. Nikparast, M. Hojatianfar, M. Akhlaghi, R. Ghorbani, and H. R. Pourianfar, "Characterisation and antifungal activity of silver nanoparticles biologically synthesised by *Amaranthus retroflexus* leaf extract," *Journal of Experimental Nanoscience*, vol. 12, no. 1, pp. 129–139, 2017.

[141] B. Yılmaz Öztürk, B. Yenice Gürsu, and İ. Dağ, "Antibiofilm and antimicrobial activities of green synthesized silver nanoparticles using marine red algae *Gelidium corneum*," *Process Biochemistry*, vol. 89, pp. 208–219, 2020.

[142] S. S. Dakshayani, M. B. Marulasiddeshwara, M. N. Sharath Kumar et al., "Antimicrobial, anticoagulant and antiplatelet activities of green synthesized silver nanoparticles using Selaginella (Sanjeevini) plant extract," *International Journal of Biological Macromolecules*, vol. 131, pp. 787–797, 2019.

[143] A.-C. Burduşel, O. Gherasim, A. M. Grumezescu, L. Mogoantă, A. Ficai, and E. Andronescu, "Biomedical applications of silver nanoparticles: an up-to-date overview," *Nanomaterials*, vol. 8, no. 9, Article ID 681, 2018.

[144] K. K. Y. Wong, S. O. F. Cheung, L. Huang et al., "Further evidence of the anti-inflammatory effects of silver nanoparticles," *ChemMedChem*, vol. 4, no. 7, pp. 1129–1135, 2009.

[145] N.-H. Nam, "Naturally occurring NF-κB inhibitors," *Mini Reviews in Medicinal Chemistry*, vol. 6, no. 8, pp. 945–951, 2006.

[146] Z. Meng, C. Yan, Q. Deng, D.-f. Gao, and X.-l. Niu, "Curcumin inhibits LPS-induced inflammation in rat vascular smooth muscle cells in vitro via ROS-relative TLR4-MAPK/NF-κB pathways," *Acta Pharmacologica Sinica*, vol. 34, no. 7, pp. 901–911, 2013.

[147] K. C. Bhol and P. J. Schechter, "Effects of nanocrystalline silver (NPI 32101) in a rat model of ulcerative colitis," *Digestive Diseases and Sciences*, vol. 52, no. 10, pp. 2732–2742, 2007.

[148] P. Singh, S. Ahn, J.-P. Kang et al., "*In vitro* anti-inflammatory activity of spherical silver nanoparticles and monodisperse hexagonal gold nanoparticles by fruit extract of *Prunus serrulata*: a green synthetic approach," *Artificial Cells, Nanomedicine, and Biotechnology*, vol. 46, no. 8, pp. 1–11, 2018.

[149] R. Vijayaraj, G. D. Kumar, and N. S. Kumaran, "*In vitro* anti-inflammatory activity of silver nanoparticle synthesized *Avicennia marina* (Forssk.) Vierh.: a green synthetic approach," *International Journal of Green Pharmacy*, vol. 10, 2018.

[150] P. Belle Ebanda Kedi, F. Eya'ane Meva, L. Kotsedi et al., "Eco-friendly synthesis, characterization, *in vitro* and *in vivo* anti-inflammatory activity of silver nanoparticle-mediated *Selaginella myosurus* aqueous extract," *International Journal of Nanomedicine*, vol. 13, pp. 8537–8548, 2018.

[151] S. Rajput, D. Kumar, and V. Agrawal, "Green synthesis of silver nanoparticles using Indian Belladonna extract and their potential antioxidant, anti-inflammatory, anticancer and larvicidal activities," *Plant Cell Reports*, vol. 39, no. 7, pp. 921–939, 2020.

[152] V. Kumar, S. Singh, B. Srivastava, R. Bhadouria, and R. Singh, "Green synthesis of silver nanoparticles using leaf extract of *Holoptelea integrifolia* and preliminary investigation of its antioxidant, anti-inflammatory, antidiabetic and antibacterial activities," *Journal of Environmental Chemical Engineering*, vol. 7, no. 3, Article ID 103094, 2019.

[153] M. Govindappa, B. Hemashekhar, M.-K. Arthikala, V. Ravishankar Rai, and Y. L. Ramachandra, "Characterization, antibacterial, antioxidant, antidiabetic, anti-inflammatory and antityrosinase activity of green synthesized silver nanoparticles using *Calophyllum tomentosum* leaves extract," *Results in Physics*, vol. 9, pp. 400–408, 2018.

[154] B. Moldovan, L. David, A. Vulcu et al., "*In vitro* and *in vivo* anti-inflammatory properties of green synthesized silver nanoparticles using *Viburnum opulus* L. fruits extract," *Materials Science and Engineering: C*, vol. 79, pp. 720–727, 2017.

[155] L. David, B. Moldovan, A. Vulcu et al., "Green synthesis, characterization and anti-inflammatory activity of silver nanoparticles using European black elderberry fruits extract," *Colloids and Surfaces B: Biointerfaces*, vol. 122, pp. 767–777, 2014.

[156] R. Williams, S. Karuranga, B. Malanda et al., *IDF Atlas*, IDF, Brussels, Belgium, 9th edition, 2019.

[157] American Diabetes Association, "Diagnosis and classification of diabetes mellitus," *Diabetes Care*, vol. 36, no. 1, pp. S67–S74, 2013.

[158] American Diabetes Association, "Classification and diagnosis of diabetes: standards of medical care in diabetes—2019," *Diabetes Care*, vol. 42, no. 1, pp. S13–S28, 2019.

[159] D. M. Nathan, "Long-term complications of diabetes mellitus," *New England Journal of Medicine*, vol. 328, no. 23, pp. 1676–1685, 1993.

[160] A. I. Martinez-Gonzalez, Á. G. Díaz-Sánchez, L. A. d. l. Rosa, C. L. Vargas-Requena, I. Bustos-Jaimes, and A. E. Alvarez-Parrilla, "Polyphenolic compounds and digestive enzymes: *in vitro* non-covalent interactions," *Molecules*, vol. 22, no. 4, p. 669, 2017.

[161] A. K. Tiwari and J. M. Rao, "Diabetes mellitus and multiple therapeutic approaches of phytochemicals: present status and future prospects," *Current Science*, vol. 83, no. 1, p. 10, 2002.

[162] M. Hanefeld, "The role of acarbose in the treatment of non-insulin-dependent diabetes mellitus," *Journal of Diabetes and Its Complications*, vol. 12, no. 4, pp. 228–237, 1998.

[163] K. Balan, W. Qing, Y. Wang et al., "Antidiabetic activity of silver nanoparticles from green synthesis using *Lonicera japonica* leaf extract," *RSC Advances*, vol. 6, no. 46, pp. 40162–40168, 2016.

[164] R. G. Saratale, H. S. Shin, G. Kumar, G. Benelli, D.-S. Kim, and G. D. Saratale, "Exploiting antidiabetic activity of silver nanoparticles synthesized using *Punica granatum* leaves and anticancer potential against human liver cancer cells (HepG2)," *Artificial Cells, Nanomedicine, and Biotechnology*, vol. 46, no. 1, pp. 211–222, 2018.

[165] K. Shanker, J. Naradala, G. K. Mohan, G. S. Kumar, and P. L. Pravallika, "A sub-acute oral toxicity analysis and comparative *in vivo* anti-diabetic activity of zinc oxide, cerium oxide, silver nanoparticles, and *Momordica charantia* in streptozotocin-induced diabetic Wistar rats," *RSC Advances*, vol. 7, no. 59, pp. 37158–37167, 2017.

[166] G. Das, J. K. Patra, T. Debnath, A. Ansari, and H.-S. Shin, "Investigation of antioxidant, antibacterial, antidiabetic, and cytotoxicity potential of silver nanoparticles synthesized using the outer peel extract of *Ananas comosus* (L.)," *PLoS One*, vol. 14, no. 8, Article ID e0220950, 2019.

[167] S. Yarrappagaari, R. Gutha, L. Narayanaswamy et al., "Eco-friendly synthesis of silver nanoparticles from the whole plant of *Cleome viscosa* and evaluation of their characterization, antibacterial, antioxidant and antidiabetic properties," *Saudi Journal of Biological Sciences*, vol. 27, no. 12, pp. 3601–3614, 2020.

[168] B. Das, A. De, S. Podder, S. Das, C. K. Ghosh, and A. Samanta, "Green biosynthesis of silver nanoparticles using *Dregea volubilis* flowers: characterization and evaluation of antioxidant, antidiabetic and antibacterial activity," *Inorganic and Nano-Metal Chemistry*, vol. 51, no. 8, pp. 1066–1079, 2020.

[169] P. Johnson, V. Krishnan, C. Loganathan et al., "Rapid biosynthesis of *Bauhinia variegata* flower extract-mediated silver nanoparticles: an effective antioxidant scavenger and α-amylase inhibitor," *Artificial Cells, Nanomedicine, and Biotechnology*, vol. 46, no. 7, pp. 1488–1494, 2018.

[170] S. K. Das, S. Behera, J. K. Patra, and H. Thatoi, "Green synthesis of sliver nanoparticles using *Avicennia officinalis* and *Xylocarpus granatum* extracts and *in vitro* evaluation of antioxidant, antidiabetic and anti-inflammatory activities," *Journal of Cluster Science*, vol. 30, no. 4, pp. 1103–1113, 2019.

[171] S. Wu, W. Zhu, P. Thompson, and Y. A. Hannun, "Evaluating intrinsic and non-intrinsic cancer risk factors," *Nature Communications*, vol. 9, no. 1, Article ID 3490, 2018.

[172] Z. A. Ratan, M. F. Haidere, M. Nurunnabi et al., "Green chemistry synthesis of silver nanoparticles and their potential anticancer effects," *Cancers*, vol. 12, no. 4, Article ID 855, 2020.

[173] G. M. Vlăsceanu, Ş. Marin, R. E. Ţiplea et al., "Silver nanoparticles in cancer therapy," in *Nanobiomaterials in Cancer Therapy*, pp. 29–56, Elsevier, Amsterdam, Netherlands, 2016.

[174] Ş. Yeşilot and Ç. A. Aydın Acar, "Silver nanoparticles; a new hope in cancer therapy?" *Eastern Journal of Medicine*, vol. 24, no. 1, pp. 111–116, 2019.

[175] M. A. Siddiquee, M. u. d. Parray, S. H. Mehdi et al., "Green synthesis of silver nanoparticles from *Delonix regia* leaf extracts: *in-vitro* cytotoxicity and interaction studies with bovine serum albumin," *Materials Chemistry and Physics*, vol. 242, Article ID 122493, 2020.

[176] P. Kuppusamy, S. J. A. Ichwan, P. N. H. Al-Zikri et al., "*In vitro* anticancer activity of Au, Ag nanoparticles synthesized using *Commelina nudiflora* L. aqueous extract against HCT-116 colon cancer cells," *Biological Trace Element Research*, vol. 173, no. 2, pp. 297–305, 2016.

[177] Y. He, X. Li, J. Wang et al., "Synthesis, characterization and evaluation cytotoxic activity of silver nanoparticles synthesized by Chinese herbal *Cornus officinalis* via environment friendly approach," *Environmental Toxicology and Pharmacology*, vol. 56, pp. 56–60, 2017.

[178] S. Deepika, C. I. Selvaraj, and S. M. Roopan, "Screening bioactivities of *Caesalpinia pulcherrima* L. Swartz and cytotoxicity of extract synthesized silver nanoparticles on HCT116 cell line," *Materials Science and Engineering: C*, vol. 106, Article ID 110279, 2020.

[179] E. S. Al-Sheddi, N. N. Farshori, M. M. Al-Oqail et al., "Anticancer potential of green synthesized silver nanoparticles using extract of *Nepeta deflersiana* against human cervical cancer cells (HeLA)," *Bioinorganic Chemistry and Applications*, vol. 2018, Article ID 9390784, 12 pages, 2018.

[180] M. M. R. Mollick, D. Rana, S. K. Dash et al., "Studies on green synthesized silver nanoparticles using *Abelmoschus esculentus* (L.) pulp extract having anticancer (*in vitro*) and antimicrobial applications," *Arabian Journal of Chemistry*, vol. 12, no. 8, pp. 2572–2584, 2019.

[181] K. Jadhav, S. Deore, D. Dhamecha et al., "Phytosynthesis of silver nanoparticles: characterization, biocompatibility studies, and anticancer activity," *ACS Biomaterials Science & Engineering*, vol. 4, no. 3, pp. 892–899, 2018.

[182] S. Khorrami, A. Zarepour, and A. Zarrabi, "Green synthesis of silver nanoparticles at low temperature in a fast pace with unique DPPH radical scavenging and selective cytotoxicity against MCF-7 and BT-20 tumor cell lines," *Biotechnology Reports*, vol. 24, Article ID e00393, 2019.

[183] S. Mostafalou and M. Abdollahi, "Pesticides and human chronic diseases: evidences, mechanisms, and perspectives," *Toxicology and Applied Pharmacology*, vol. 268, no. 2, pp. 157–177, 2013.

[184] M. Brouwer, A. Huss, M. van der Mark et al., "Environmental exposure to pesticides and the risk of Parkinson's disease in The Netherlands," *Environment International*, vol. 107, pp. 100–110, 2017.

[185] C. Freire, R. J. Koifman, P. N. Sarcinelli, A. C. Simões Rosa, R. Clapauch, and S. Koifman, "Long-term exposure to organochlorine pesticides and thyroid status in adults in a heavily contaminated area in Brazil," *Environmental Research*, vol. 127, pp. 7–15, 2013.

[186] S. R. Kirkhorn and M. B. Schenker, "Current health effects of agricultural work: respiratory disease, cancer, reproductive effects, musculoskeletal injuries, and pesticide–related illnesses," *Journal of Agricultural Safety and Health*, vol. 8, no. 2, pp. 199–214, 2002.

[187] G. Suresh, P. H. Gunasekar, D. Kokila et al., "Green synthesis of silver nanoparticles using *Delphinium denudatum* root extract exhibits antibacterial and mosquito larvicidal activities," *Spectrochimica Acta Part A: Molecular and Biomolecular Spectroscopy*, vol. 127, pp. 61–66, 2014.

[188] A. Fouda, S. E.-D. Hassan, A. M. Abdo, and M. S. El-Gamal, "Antimicrobial, antioxidant and larvicidal activities of spherical silver nanoparticles synthesized by endophytic streptomyces spp," *Biological Trace Element Research*, vol. 195, no. 2, pp. 707–724, 2020.

[189] T. Y. Suman, D. Elumalai, P. K. Kaleena, and S. R. R. Rajasree, "GC-MS analysis of bioactive components and synthesis of silver nanoparticle using *Ammannia baccifera* aerial extract and its larvicidal activity against malaria and filariasis vectors," *Industrial Crops and Products*, vol. 47, pp. 239–245, 2013.

[190] A. Rawani, A. Ghosh, and G. Chandra, "Mosquito larvicidal and antimicrobial activity of synthesized nano-crystalline silver particles using leaves and green berry extract of *Solanum nigrum* L. (Solanaceae: Solanales)," *Acta Tropica*, vol. 128, no. 3, pp. 613–622, 2013.

[191] D. Elumalai, M. Hemavathi, C. V. Deepaa, and P. K. Kaleena, "Evaluation of phytosynthesised silver nanoparticles from leaf extracts of *Leucas aspera* and *Hyptis suaveolens* and their larvicidal activity against malaria, dengue and filariasis vectors," *Parasite Epidemiology and Control*, vol. 2, no. 4, pp. 15–26, 2017.

[192] M. Govindarajan, M. Rajeswary, K. Veerakumar, U. Muthukumaran, S. L. Hoti, and G. Benelli, "Green synthesis and characterization of silver nanoparticles fabricated using *Anisomeles indica*: mosquitocidal potential against malaria, dengue and Japanese encephalitis vectors," *Experimental Parasitology*, vol. 161, pp. 40–47, 2015.

[193] E. Parthiban, N. Manivannan, R. Ramanibai, and N. Mathivanan, "Green synthesis of silver-nanoparticles from *Annona reticulata* leaves aqueous extract and its mosquito larvicidal and anti-microbial activity on human pathogens," *Biotechnology Reports*, vol. 21, Article ID e00297, 2019.

[194] U. Muthukumaran, M. Govindarajan, M. Rajeswary, and S. L. Hoti, "Synthesis and characterization of silver nanoparticles using *Gmelina asiatica* leaf extract against filariasis, dengue, and malaria vector mosquitoes," *Parasitology Research*, vol. 114, no. 5, pp. 1817–1827, 2015.

[195] X. Zuo, K. Chang, J. Zhao et al., "Bubble-template-assisted synthesis of hollow fullerene-like MoS_2 nanocages as a

lithium ion battery anode material," *Journal of Materials Chemistry*, vol. 4, no. 1, pp. 51–58, 2016.

[196] C. J. Li and X. Bi, *Silver Catalysis in Organic Synthesis*, Wiley, Hoboken, NJ, USA, 1st edition, 2019.

[197] A. Arya, V. Mishra, and T. S. Chundawat, "Green synthesis of silver nanoparticles from green algae (*Botryococcus braunii*) and its catalytic behavior for the synthesis of benzimidazoles," *Chemical Data Collections*, vol. 20, Article ID 100190, 2019.

[198] C. Shanmugam, G. Sivasubramanian, B. Parthasarathi, K. Baskaran, R. Balachander, and V. R. Parameswaran, "Antimicrobial, free radical scavenging activities and catalytic oxidation of benzyl alcohol by nano-silver synthesized from the leaf extract of *Aristolochia indica* L.: a promenade towards sustainability," *Applied Nanoscience*, vol. 6, no. 5, pp. 711–723, 2016.

[199] W. H. Eisa, M. F. Zayed, B. Anis, L. M. Abbas, S. S. M. Ali, and A. M. Mostafa, "Clean production of powdery silver nanoparticles using *Zingiber officinale*: the structural and catalytic properties," *Journal of Cleaner Production*, vol. 241, Article ID 118398, 2019.

[200] P. K. Gogoi, T. Begum, B. Borthakur, G. Das, U. Bora, and A. Kumar, "Green synthesis of silver nanoparticles using leaf extract of *Phlogacanthus thyrsiformis* and evaluation of their antibacterial and catalytic activity," *National Academy Science Letters*, vol. 38, no. 3, pp. 231–234, 2015.

[201] M. Nasrollahzadeh, F. Babaei, S. Mohammad Sajadi, and A. Ehsani, "Green synthesis, optical properties and catalytic activity of silver nanoparticles in the synthesis of N-monosubstituted ureas in water," *Spectrochimica Acta Part A: Molecular and Biomolecular Spectroscopy*, vol. 132, pp. 423–429, 2014.

[202] H. Veisi, S. Azizi, and P. Mohammadi, "Green synthesis of the silver nanoparticles mediated by *Thymbra spicata* extract and its application as a heterogeneous and recyclable nanocatalyst for catalytic reduction of a variety of dyes in water," *Journal of Cleaner Production*, vol. 170, pp. 1536–1543, 2018.

[203] S. G. Balwe, V. V. Shinde, A. A. Rokade, S. S. Park, and Y. T. Jeong, "Green synthesis and characterization of silver nanoparticles (Ag NPs) from extract of plant *Radix Puerariae*: an efficient and recyclable catalyst for the construction of pyrimido[1,2-b]indazole derivatives under solvent-free conditions," *Catalysis Communications*, vol. 99, pp. 121–126, 2017.

[204] M. A. Hossain, P. Piyatida, J. A. T. da Silva, and M. Fujita, "Molecular mechanism of heavy metal toxicity and tolerance in plants: central role of glutathione in detoxification of reactive oxygen species and methylglyoxal and in heavy metal chelation," *Journal of Botany*, vol. 2012, Article ID 872875, 37 pages, 2012.

[205] B. Lellis, C. Z. Fávaro-Polonio, J. A. Pamphile, and J. C. Polonio, "Effects of textile dyes on health and the environment and bioremediation potential of living organisms," *Biotechnology Research and Innovation*, vol. 3, no. 2, pp. 275–290, 2019.

[206] B. Neppolian, H. C. Choi, S. Sakthivel, B. Arabindoo, and V. Murugesan, "Solar/UV-induced photocatalytic degradation of three commercial textile dyes," *Journal of Hazardous Materials*, vol. 89, no. 2, pp. 303–317, 2002.

[207] Y. Ma, Q. Ding, L. Yang, L. Zhang, and Y. Shen, "Ag nanoparticles as multifunctional SERS substrate for the adsorption, degradation and detection of dye molecules," *Applied Surface Science*, vol. 265, pp. 346–351, 2013.

[208] V. K. Gupta, R. Jain, and S. Varshney, "Electrochemical removal of the hazardous dye reactofix red 3 BFN from industrial effluents," *Journal of Colloid and Interface Science*, vol. 312, no. 2, pp. 292–296, 2007.

[209] Y. Wang, L. Gai, W. Ma, H. Jiang, X. Peng, and L. Zhao, "Ultrasound-assisted catalytic degradation of methyl orange with Fe_3O_4/polyaniline in near neutral solution," *Industrial & Engineering Chemistry Research*, vol. 54, no. 8, pp. 2279–2289, 2015.

[210] L. David and B. Moldovan, "Green synthesis of biogenic silver nanoparticles for efficient catalytic removal of harmful organic dyes," *Nanomaterials*, vol. 10, no. 2, p. 202, 2020.

[211] W. Qing, K. Chen, Y. Wang, X. Liu, and M. Lu, "Green synthesis of silver nanoparticles by waste tea extract and degradation of organic dye in the absence and presence of H_2O_2," *Applied Surface Science*, vol. 423, pp. 1019–1024, 2017.

[212] V. Srivastava, S. Pandey, A. Mishra, and A. K. Choubey, "Green synthesis of biogenic silver particles, process parameter optimization and application as photocatalyst in dye degradation," *SN Applied Sciences*, vol. 1, no. 12, Article ID 1722, 2019.

[213] K. Anand, K. Kaviyarasu, S. Muniyasamy, S. M. Roopan, R. M. Gengan, and A. A. Chuturgoon, "Bio-synthesis of silver nanoparticles using agroforestry residue and their catalytic degradation for sustainable waste management," *Journal of Cluster Science*, vol. 28, no. 4, pp. 2279–2291, 2017.

[214] B. Khodadadi, M. Bordbar, A. Yeganeh-Faal, and M. Nasrollahzadeh, "Green synthesis of Ag nanoparticles/clinoptilolite using *Vaccinium macrocarpon* fruit extract and its excellent catalytic activity for reduction of organic dyes," *Journal of Alloys and Compounds*, vol. 719, pp. 82–88, 2017.

[215] N. N. Bonnia, M. S. Kamaruddin, M. H. Nawawi, S. Ratim, H. N. Azlina, and E. S. Ali, "Green biosynthesis of silver nanoparticles using "*Polygonum Hydropiper*" and study its catalytic degradation of methylene blue," *Procedia Chemistry*, vol. 19, pp. 594–602, 2016.

[216] S. Joseph and B. Mathew, "Microwave-assisted green synthesis of silver nanoparticles and the study on catalytic activity in the degradation of dyes," *Journal of Molecular Liquids*, vol. 204, pp. 184–191, 2015.

[217] M. Mosaviniya, T. Kikhavani, M. Tanzifi, M. Tavakkoli Yaraki, P. Tajbakhsh, and A. Lajevardi, "Facile green synthesis of silver nanoparticles using *Crocus Haussknechtii* Bois bulb extract: catalytic activity and antibacterial properties," *Colloid and Interface Science Communications*, vol. 33, Article ID 100211, 2019.

[218] T. Varadavenkatesan, R. Vinayagam, and R. Selvaraj, "Green synthesis and structural characterization of silver nanoparticles synthesized using the pod extract of *Clitoria ternatea* and its application towards dye degradation," *Materials Today Proceedings*, vol. 23, pp. 27–29, 2020.

[219] G. Azeh Engwa, P. Udoka Ferdinand, F. Nweke Nwalo, and M. N. Unachukwu, "Mechanism and health effects of heavy metal toxicity in humans," *Poisoning in the Modern World-New Tricks for an Old Dog?*, Intechopen, London, UK, 2019.

[220] K. S. Squibb and B. A. Fowler, "Relationship between metal toxicity to subcellular systems and the carcinogenic response," *Environmental Health Perspectives*, vol. 40, pp. 181–188, 1981.

[221] P. Koedrith and Y. R. Seo, "Advances in carcinogenic metal toxicity and potential molecular markers," *International Journal of Molecular Sciences*, vol. 12, no. 12, pp. 9576–9595, 2011.

[222] A. Helaluddin, R. S. Khalid, M. Alaama, and S. A. Abbas, "Main analytical techniques used for elemental analysis in various matrices," *Tropical Journal of Pharmaceutical Research*, vol. 15, no. 2, p. 427, 2016.

[223] A. D. McFarland and R. P. Van Duyne, "Single Silver nanoparticles as real-time optical sensors with zeptomole sensitivity," *Nano Letters*, vol. 3, no. 8, pp. 1057–1062, 2003.

[224] L. E. Silva-De Hoyos, V. Sánchez-Mendieta, A. R. Vilchis-Nestor, and M. A. Camacho-López, "Biogenic silver nanoparticles as sensors of Cu^{2+} and Pb^{2+} in aqueous solutions," *Universal Journal of Materials Science*, vol. 5, no. 2, pp. 29–37, 2017.

[225] M. Ihsan, A. Niaz, A. Rahim et al., "Biologically synthesized silver nanoparticle-based colorimetric sensor for the selective detection of Zn^{2+}," *RSC Advances*, vol. 5, no. 111, pp. 91158–91165, 2015.

[226] C. K. Balavigneswaran, T. Sujin Jeba Kumar, R. Moses Packiaraj, and S. Prakash, "Rapid detection of Cr(VI) by AgNPs probe produced by *Anacardium occidentale* fresh leaf extracts," *Applied Nanoscience*, vol. 4, no. 3, pp. 367–378, 2014.

[227] M. F. Zayed, W. H. Eisa, S. M. El-kousy, W. K. Mleha, and N. Kamal, "*Ficus retusa*-stabilized gold and silver nanoparticles: controlled synthesis, spectroscopic characterization, and sensing properties," *Spectrochimica Acta Part A: Molecular and Biomolecular Spectroscopy*, vol. 214, pp. 496–512, 2019.

[228] C. J. Kirubaharan, D. Kalpana, Y. S. Lee et al., "Biomediated silver nanoparticles for the highly selective copper(II) Ion sensor applications," *Industrial & Engineering Chemistry Research*, vol. 51, no. 21, pp. 7441–7446, 2012.

[229] S. K. Chandraker, M. K. Ghosh, M. Lal, T. K. Ghorai, and R. Shukla, "Colorimetric sensing of Fe^{3+} and Hg^{2+} and photocatalytic activity of green synthesized silver nanoparticles from the leaf extract of *Sonchus arvensis* L." *New Journal of Chemistry*, vol. 43, no. 46, pp. 18175–18183, 2019.

[230] A. Aravind, M. Sebastian, and B. Mathew, "Green silver nanoparticles as a multifunctional sensor for toxic Cd(ii) ions," *New Journal of Chemistry*, vol. 42, no. 18, pp. 15022–15031, 2018.

[231] A. Aravind, M. Sebastian, and B. Mathew, "Green synthesized unmodified silver nanoparticles as a multi-sensor for Cr(iii) ions," *Environmental Sciences: Water Research & Technology*, vol. 4, no. 10, pp. 1531–1542, 2018.

[232] Z. Ferdous and A. Nemmar, "Health impact of silver nanoparticles: a review of the biodistribution and toxicity following various routes of exposure," *International Journal of Molecular Sciences*, vol. 21, no. 7, Article ID 2375, 2020.

[233] J. N. Smith, D. G. Thomas, H. Jolley et al., "All that is silver is not toxic: silver ion and particle kinetics reveals the role of silver ion aging and dosimetry on the toxicity of silver nanoparticles," *Particle and Fibre Toxicology*, vol. 15, no. 1, p. 47, 2018.

[234] T. Tolaymat, A. El Badawy, A. Genaidy, W. Abdelraheem, and R. Sequeira, "Analysis of metallic and metal oxide nanomaterial environmental emissions," *Journal of Cleaner Production*, vol. 143, pp. 401–412, 2017.

[235] F. Seitz, R. R. Rosenfeldt, K. Storm et al., "Effects of silver nanoparticle properties, media pH and dissolved organic matter on toxicity to *Daphnia magna*," *Ecotoxicology and Environmental Safety*, vol. 111, pp. 263–270, 2015.

[236] R. Ishwarya, B. Vaseeharan, S. Shanthi et al., "Green synthesized silver nanoparticles: toxicity against *Poecilia reticulata* Fishes and *Ceriodaphnia cornuta* Crustaceans," *Journal of Cluster Science*, vol. 28, no. 1, pp. 519–527, 2017.

[237] A. A. Jenifer, B. Malaikozhundan, S. Vijayakumar, M. Anjugam, A. Iswarya, and B. Vaseeharan, "Green synthesis and characterization of silver nanoparticles (AgNPs) using leaf extract of *Solanum nigrum* and assessment of toxicity in vertebrate and invertebrate aquatic animals," *Journal of Cluster Science*, vol. 31, no. 5, pp. 989–1002, 2020.

[238] D. T. Rheder, M. Guilger, N. Bilesky-José et al., "Synthesis of biogenic silver nanoparticles using *Althaea officinalis* as reducing agent: evaluation of toxicity and ecotoxicity," *Scientific Reports*, vol. 8, no. 1, Article ID 12397, 2018.

[239] T. Santhoshkumar, A. A. Rahuman, G. Rajakumar et al., "Synthesis of silver nanoparticles using *Nelumbo nucifera* leaf extract and its larvicidal activity against malaria and filariasis vectors," *Parasitology Research*, vol. 108, no. 3, pp. 693–702, 2011.

[240] M. Khoshnamvand, Z. Hao, O. O. Fadare, P. Hanachi, Y. Chen, and J. Liu, "Toxicity of biosynthesized silver nanoparticles to aquatic organisms of different trophic levels," *Chemosphere*, vol. 258, Article ID 127346, 2020.

[241] C. Krishnaraj, S. L. Harper, and S.-I. Yun, "*In vivo* toxicological assessment of biologically synthesized silver nanoparticles in adult zebrafish (*Danio rerio*)," *Journal of Hazardous Materials*, vol. 301, pp. 480–491, 2016.

[242] C. Shobana, B. Rangasamy, R. K. Poopal, S. Renuka, and M. Ramesh, "Green synthesis of silver nanoparticles using *Piper nigrum*: tissue-specific bioaccumulation, histopathology, and oxidative stress responses in Indian major carp *Labeo rohita*," *Environmental Science and Pollution Research*, vol. 25, no. 12, pp. 11812–11832, 2018.